

**EFFECTS OF NUTRIENT SUPPLY ON METABOLIC RATES
IN THE OLIGOTROPHIC OCEAN:
INSIGHTS FROM A LONG-TERM AND LARGE-SCALE INCUBATION EXPERIMENT**

A THESIS SUBMITTED TO THE GRADUATE DIVISION OF THE
UNIVERSITY OF HAWAI‘I AT MĀNOA IN PARTIAL FULFILLMENT
OF THE REQUIREMENTS FOR THE DEGREE OF

MASTER OF SCIENCE

IN

OCEANOGRAPHY

AUGUST 2022

By
Andrés Esteban Salazar Estrada

Thesis Committee:

Sara Ferrón, Chairperson
Kyle F. Edwards
David M. Karl

CONTENTS

ACKNOWLEDGEMENTS	iii
----------------------------	-----

ABSTRACT	iv
--------------------	----

INTRODUCTION

OCEANIC PRIMARY PRODUCTION AND RESPIRATION	1
NUTRIENT SUPPLY AND PRODUCTION	2
STUDY AREA: NORTH PACIFIC SUBTROPICAL GYRE	4

MATERIALS AND METHODS

EXPERIMENTAL DESIGN	5
SAMPLE COLLECTION AND INCUBATIONS	7
MEMBRANE-INLET MASS SPECTROMETRY	9
RATE CALCULATIONS	9
STATISTICAL ANALYSIS	12

RESULTS

GROSS OXYGEN PRODUCTION	13
DAYTIME LIGHT AND DARK RESPIRATION	15
NET OXYGEN CHANGE IN THE LIGHT	18

DISCUSSION

EFFECTS OF NITROGEN SUPPLY	21
EFFECTS OF PHOSPHORUS AND IRON SUPPLY	24
PATTERNS IN LIGHT AND DARK RESPIRATION	26

CONCLUSIONS	30
-----------------------	----

REFERENCES	31
----------------------	----

APPENDIX

COMPLEMENTARY MEASUREMENTS	
INORGANIC NUTRIENTS	38
CHLOROPHYLL	41

FIGURES

1) Figure 1: Daily means of metabolic rates	15
2) Figure 2: Gross Oxygen Production rates for treatments without N	16
3) Figure 3: Metabolic rates comparisons	17
4) Figure 4: Respiration comparisons	18
5) Figure 5: Estimated diel Net Community Production	19
6) Figure A1: Daily means of chlorophyll concentrations	39
7) Figure A2: Comparison between Gross Oxygen Production and chlorophyll	40
8) Figure A3: Daily means of production to chlorophyll ratios	41
9) Figure A4: Daily means of inorganic nutrient concentrations	43

TABLES

1) Table 1: Sampling and incubation schedule	7
2) Table 2: Metabolic rates dataset summary	11
3) Table 3: Collection day data	13
4) Table 4: Statistical analyses	19
5) Table A1: List of collaborating institutions, groups, and samples requested	34

Acknowledgements

First, I would like to thank the PERI-SCOPE team and the John Lab at USC, especially Emily Seelen and Emily Townsend, for being the backbone of PERI-FIX and materializing this amazing collaborative research experience that I am privileged to be a part of.

I would also like to extend a thank you to the sources of my graduate assistantship funding: the Simons Collaboration on Ocean Processes and Ecology, and The Metals Company.

My research achievements during my graduate studies are in large part due to the incredible support from my advisor. Thank you for always being there for me, Sara. I also appreciate the rest of my committee, Dave and Kyle, for their invaluable advice when it was most needed.

Everyone in the Oceanography, HOT, and CMORE ‘ohana has left a mark in me during my time here that is meaningful to me no matter how small. I appreciate our community and their support, especially from the Ocean Office staff who are always working tirelessly for the benefit of our students.

Finalmente, le mando todo mi cariño y gratitud a mi familia y seres queridos en Chile y el mundo. Sin su amor y apoyo a través de mi vida no habría logrado esto. Para mí, esto también es su logro, y siempre se los agradeceré.

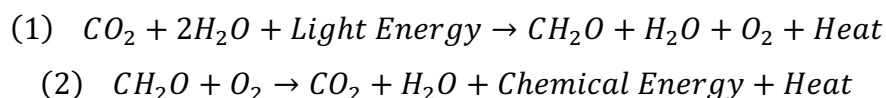
Abstract

Phytoplankton in the surface ocean account for nearly half of all the primary production on Earth, while accounting for less than 1% of terrestrial plant biomass. This outsized importance makes determining the rates at which organic matter is produced and consumed in the surface ocean paramount to constraining the global carbon cycle. To understand the effects of nutrient supply and nutrient supply ratio on oligotrophic microbial communities, a collaborative, long-term (30 days) manipulation experiment was undertaken in Honolulu, Hawai'i. Between August and September of 2021, 24 large scale (~120 L) incubators were provided with 7 daily nutrient addition treatments, plus a control, in triplicate, while monitoring the rates of gross oxygen production (GOP), daytime respiration in the light (LR), daytime respiration in the dark (DR), and net oxygen change (NOC). Our results show significant increases in GOP (9 to 14-fold) for the treatments provided with inorganic nitrogen, as well as a shift to more autotrophic conditions. The addition of inorganic phosphorus had a much smaller but noticeable effect in GOP during the experiment, suggesting the possible enhancement of photosynthesis by N₂-fixation. The addition of iron did not show any significant effect on metabolic rates. LR was estimated to be on average 30% greater than DR measurements throughout the experiment—with the difference between the two increasing with GOP. The difference between both estimates of respiration could be indicative of diel variations in community respiration, which has implications for properly constraining the carbon cycle in aquatic ecosystems.

Introduction

Oceanic Primary Production and Respiration

Oxygenic photosynthesis and aerobic cellular respiration are the two most fundamental sets of metabolic processes in the global biosphere. Photosynthesis (Eq. 1) allows autotrophs to use solar energy for reducing carbon dioxide (CO₂) into organic matter (CH₂O) for energy storage, growth, and reproduction. Aerobic respiration (Eq. 2), by both autotrophs and heterotrophs, in turn uses oxygen (O₂) to oxidize this organic matter and provide chemical energy that can be used in further anabolic processes. With these two processes being cardinal in biological carbon cycling, constraining their fluxes is paramount to understanding the global carbon cycle in the present and future.



Global estimates show that nearly half of the Earth's annual primary production occurs in the oceans, yet marine phytoplankton in surface waters account for less than 1% of land plant biomass (Bar-On et al., 2018; Field et al., 1998). This difference in standing biomass highlights the relevance of the vertical dimension of the oceans, where organic matter can be exported to depths beyond the euphotic zone and be sequestered away from the atmosphere for hundreds to thousands of years (Henson et al., 2011; Siegenthaler & Sarmiento, 1993). This biological carbon pump is a major component of the oceanic carbon cycling; an important mediator in the sink of atmospheric CO₂ of particular importance when anthropogenic fossil fuel combustion has no end in sight. Perturbations to the biological carbon pump could alter not only the global carbon cycle but also Earth's climate (Henson et al., 2011; Siegenthaler & Sarmiento, 1993). One way to empirically assess the strength of the biological carbon pump is to calculate the difference between organic matter production and consumption in the upper ocean—that

is, the balance between the rates of plankton primary production and respiration in the euphotic zone. This metabolic balance between gross primary production and community respiration is deemed net community production (NCP), and when integrated over long spatial and temporal scales it approximates carbon export from the euphotic zone (Emerson, 2014).

Aerobic respiration is commonly measured as O₂ consumed in the dark (Eq. 2; Robinson & Williams, 2005), while oceanic primary production has been measured through various methods that try to constrain either the amount of carbon fixed, or the amount of oxygen produced (Church et al., 2019). These methods range from cellular scale to remote sensing approaches, with the latter example being instrumental in assessing the global distribution of oceanic productivity through photosynthetic pigments (Falkowski & Raven, 2007). Ocean color-derived biomass estimates show that roughly three-quarters of the world's surface ocean is oligotrophic: low productivity surface waters with chlorophyll *a* concentrations below 1 mg m⁻³ (Antoine et al., 1996). Partly because of the small magnitude of oligotrophic primary productivity and respiration rates—with the balance between them being around an order of magnitude smaller—quantifying oligotrophic NCP is a contemporary challenge. Therefore, the metabolic status of surface oligotrophic regions has been debated at length (Duarte et al., 2013; Ducklow & Doney, 2013; Williams et al., 2013).

Nutrient supply and production

The geography of primary productivity and phytoplankton biomass is tightly coupled with the availability of essential nutrients, but the theory has gone beyond the explicit terms in the simplified production equation (Eq.1), as the understanding of the relationship between nutrient supply and productivity has changed significantly in the last century. In 1958, Alfred Redfield showed that the stoichiometry of surface plankton was consistent with the stoichiometry of dissolved nutrients in deeper waters (Redfield, 1958). He proposed that phytoplankton determine ocean chemistry through

their exported biomass, with a C:N:P ratio of 106:16:1 for both phytoplankton and zooplankton. In other words, this theory proposed that the elemental composition of exported remineralized dissolved nutrients maintain the uptake ratios determined by phytoplankton, suggesting a universal uptake ratio dubbed the “Redfield ratio.” This ratio became a tenet for both biological and geochemical oceanographers, and has been used to frame phytoplankton biogeochemistry, including in calculations of productivity and organic matter export (Lenton et al., 2014; Shaffer, 1996).

However, these theories regarding static cellular and environmental ratios have been questioned empirically, with experiments showing variability in C:N:P ratios not only by species and growth stage, but also seasonally and geographically (Geider & la Roche, 2002; Martiny et al., 2013; Moreno & Martiny, 2018). These ratios have been shown to be especially plastic under low nutrient availability. In this regard, oligotrophic gyres are known to be more stratified in the summer compared to winter, which limits the vertical supply of macronutrients, producing higher C:N, C:P, and N:P ratios in the summer/fall and lower ratios in the winter/spring. These nutrient starved regions favor the presence of diazotrophs, microorganisms that are capable of fixing N_2 in these N-limited systems (Karl et al., 2002). However, N_2 -fixation is an energy demanding process, and generally makes diazotrophs have slower maximum growth rates compared to non-diazotrophs. Theoretically, this means that to produce nitrogenase—the enzyme required to split the triple bond in N_2 —and competitively coexist with non-diazotrophs, there needs to be excess phosphorus and iron while non-diazotrophs need to be limited by nitrogen (Dutkiewicz et al., 2012, 2014; Tilman et al., 1982; Tilman David, 1977; Ward et al., 2013). Yet, there is still a need for empirically assessing these resource ratio theories in natural microbial communities.

Study area: NPSG

Deemed the largest uninterrupted biome in the world at roughly 20 million km² in area, the North Pacific Subtropical Gyre (NPSG) is one of the nutrient-starved regions of the world's ocean (Sverdrup et al., 1942). The surface waters of the NPSG are consistently oligotrophic because they lack nutrient delivery from land as well as from deeper nutrient-rich waters. This subtropical region is characterized by year-round warm surface waters (> 24 °C) which create a permanent low-density cap that isolates the mixed layer (~0-40 m) from the water column below 60 meters (Karl & Church, 2014). Because of this strong and persistent stratification, the NPSG was long considered a relatively stable and homogeneous, low-productivity ecosystem. Yet, continued research over the last several decades, particularly since the establishment of the Hawaii Ocean Time-series program in 1988 (Karl & Lukas, 1996), has shown variability in community composition, primary production, particulate matter export, and nutrient limitation from seasonal to interdecadal timescales (e.g., Dore et al., 2003, 2009; Karl et al., 2001a, 2021; Letelier et al., 2019). Of particular interest in the NPSG are frequent yet aperiodic phytoplankton blooms thought to be driven by diazotrophs. These blooms signify a large input of new N into the system and have a significant effect in the new production of the NPSG, where N₂ fixation accounts for nearly half of the nitrogen exported to deeper waters (Dore et al., 2002; Karl et al., 1997, 2021). Although some of this variability is thought to be climate-driven, the mechanisms that effect these changes in the microbial communities are not well understood.

To test whether an increased Fe to N and P to N supply ratio would induce diazotroph growth as predicted by resource ratio theory, a group of scientists from the Simons Collaboration on Ocean Processes and Ecology (SCOPE) program led by principal investigator Seth John (University of Southern California) designed an experiment using a set of relatively large-scale (120 L) Pelagic Ecosystem Research Incubators (PERIcosms), within the NPSG. In August and September of 2021, a large-scale and long-term (30 days) PERI-SCOPE nutrient manipulation experiment was conducted in

O‘ahu, Hawai‘i, to investigate the shifts in microbial ecology from oligotrophic surface waters of the NPSG under altered nutrient supply regimes. As part of this collaboration, the research presented herein aimed to specifically study the impacts of nutrient supply to plankton metabolic rates by tracking changes in gross oxygen production (GOP), net oxygen change (NOC), and respiration of plankton communities throughout the experiment in ~6-hour daytime incubations.

Materials and Methods

Experimental Design

This research is part of a larger collaborative effort within the SCOPE program (<http://scope.soest.hawaii.edu/>), through the PERI-SCOPE project. The first experiment, PERI-FIX (Fe Incubation eXperiment), was conducted in August–September 2021, at the University of Hawaii’s Marine Center (UHMC) in Honolulu. The main goal of PERI-FIX was to maintain natural oligotrophic microbial communities in relatively large scale incubators for multiple weeks, while manipulating their N:P:Fe supply to evaluate the impacts of changes in nutrient supply ratio on microbial community structure, physiology, and metabolism. Of particular interest was testing the hypothesis of phosphorus and iron limitation in diazotrophs.

Whole surface seawater was collected at nighttime 13 miles off the southern coast of Oahu (21.10° N, 158.06° W; collection depth: ~5m; location depth >800m) in nine 275-gallons totes (> 11,000 L), using an air operated double-diaphragm (AODD) pump under trace metal clean conditions. Once back at the UHMC, seawater from 4 totes was aliquoted into 24 trace-metal clean PERIcosms using an AODD pump. The rest of the seawater collected was used to refill the microcosms after each sampling event by filtering it through an AcroPak™ capsule with a 0.2 µm PES Supor membrane (Pall Corporation).

The PERIcosms were located inside an air conditioned and HEPA-filtered tent for the duration of the experiment.

The PERIcosms consisted of 120-liter, fully enclosed medium-density polyethylene inductor tanks with multiple sampling ports, a fill port, a spike port, a sediment trap located at the bottom to collect settled particles, and an automated light source at the top (Kessil A360X Refugium lights)—all for maintaining and tracking the collected microbial community. The PERIcosms were maintained on a 13-hour light:11-hour dark diurnal cycle around 06:00–19:00 hrs. When lights were on, photosynthetically active radiation inside the tanks ranged between 40–300 $\mu\text{mol m}^{-2} \text{s}^{-1}$ within the tank's vertical water column.

The 24 PERIcosms were treated with eight nutrient regimes in triplicate, with nitrogen (N), phosphorus (P), and iron (F) being the three inorganic nutrients selected for manipulation in this experiment. These eight treatments come from Boolean combinations of the addition of each nutrient: N, P, F, NP, NF, NPF, PF, and a control (C) treatment with no nutrients added. Nutrient addition occurred daily: N tanks were spiked with 75 $\text{nmol L}^{-1} \text{day}^{-1}$ of each NaNO_3 and NH_4Cl , for a total of 150 $\text{nmol L}^{-1} \text{day}^{-1}$ of inorganic N; P tanks were spiked with 9.5 $\text{nmol L}^{-1} \text{day}^{-1}$ of Na_2HPO_4 ; F tanks were provided with 1 $\text{nmol L}^{-1} \text{day}^{-1}$ of FeCl_3 . There were only two days throughout the experiment where none of the PERIcosms were spiked with nutrients, on August 13th and 14th.

Tracking of the microbial communities and biogeochemistry inside the enclosures was done through direct subsampling each PERIcosm. As this was a collaborative effort, a sampling schedule was designed to fit multiple, weekly measurements while trying to avoid excessive sampling that could affect the PERIcosms' communities (e.g., continuously flushing out microorganisms through oversampling). In addition to our rate measurements, several other measurements were conducted by

different labs (Table A1), thus, during small and large biweekly sampling events, approximately 6% and 22% of each tanks' volume was replaced with filtered seawater from the remaining totes, respectively.

Table 1: Dates and times of sampling of the PERIcosms as well as the start times, end times, and durations of the bottle incubations for the determination of metabolic rates throughout PERI-FIX. All dates and times are in Hawaiian Standard Time (UTC -10 hours).

Exp. Day	Date	Sampling Start–End	Incubation Start–End	Length
1*	9 – August – 2022	12:00 – 12:30	12:52 – 17:58	5 hrs. 6 min.
3	11 – August – 2022	9:45 – 11:00	12:54 – 18:50	5 hrs. 56 min.
5	13 – August – 2022	8:18 – 9:42	12:10 – 18:15	6 hrs. 5 min.
8	16 – August – 2022	8:30 – 9:30	11:51 – 17:51	6 hrs.
12	20 – August – 2022	8:34 – 9:32	12:03 – 18:05	6 hrs. 2 min
15	23 – August – 2022	9:24 – 10:26	12:40 – 18:45	6 hrs. 5 min.
19	27 – August – 2022	9:40 – 10:10	12:45 – 18:50	6 hrs. 5 min.
22	30 – August – 2022	9:26 – 10:12	12:48 – 18:50	6 hrs. 2 min
26	3 – August – 2022	8:55 – 9:45	12:12 – 18:56	6 hrs. 44 min
30	7 – August – 2022	8:25 – 9:00	11:40 – 18:50	7 hrs. 10 min.

*Samples were collected from the collection totes in this day

Sample Collection and Incubation Experiments

Every Monday and Friday throughout the duration of the experiment, as well as the Wednesday of the first week (10 sampling days total; Table 1), we sub-sampled every PERIcosms for the determination gross oxygen productivity by the ^{18}O -H₂O method as described in Ferrón et al. (2016). The net oxygen change was determined in bottles incubated both in the light and in the dark, for the calculation of respiration.

Water was collected from each PERIcosm in 1-liter polycarbonate bottles and then siphoned with silicone tubing into three 130-mL Pyrex® bottles with ground-glass joints and flat-bottom stoppers.

One bottle was used as the reference for the initial, pre-incubation conditions, and was called the “time-

zero” bottle. The second one—referred to as the “light” bottle—was spiked using a pipette with 650 μL of H_2^{18}O (Medical Isotopes, 97% isotopic purity) to a final ^{18}O - H_2O enrichment of $\sim 2400\text{‰}$, and then incubated for the determination of GOP, NOC, and daytime respiration in the light. The third bottle was incubated under dark conditions for the determination of daytime respiration in the dark and referred to as the “dark” bottle. All glass bottles were kept away from direct light sources during sampling and handled in low light conditions while outside of the incubation.

Once all PERIcosms were siphoned for a total of 72 Pyrex® bottles, the “time-zero” bottles were first fixed by pipetting 100 μL of saturated mercuric chloride solution to stop all biological activity and preserve the initial dissolved gas concentrations. During this step, the flat-bottom stoppers were replaced by pointed ground glass stoppers which allowed closing the bottles without introducing bubbles. The new stopper was taped shut using electrical tape, inverted at least three times to ensure proper fixing, and stored upside-down with the ground joint submerged in deionized water, at room temperature and protected from light. After fixing the “time-zero” bottles the incubations were initiated and the “light” and “dark” bottles were incubated in a water bath inside the PERI-FIX tent by the PERIcosms to ensure similar temperature conditions. The “light” bottles were placed in an uncovered water bath with the same light source as the tanks, while the “dark” bottles were placed in a covered water bath in the dark. After approximately 6 hours (Table 1), the “light” and “dark” incubations were terminated in the same manner as the “time-zero” bottles: fixing with mercuric chloride, changing stoppers without bubbles, and gently mixing before storing them upside-down with the ground joints submerged in deionized water in a covered box at room temperature. All fixed samples were stored in the dark in this way until analysis within 48 hours of fixing.

Membrane-inlet Mass Spectrometry (MIMS)

The mass-per-charge ratios (m/z) of dissolved gases—most importantly $^{32}\text{O}_2$, $^{34}\text{O}_2$ (produced by photosynthesis from the splitting of ^{18}O -water), and ^{40}Ar —were determined by Membrane Inlet Mass Spectrometry (MIMS; Ferrón et al., 2016; Kana et al., 1994) within 48 hours of the end of the incubations. Briefly, the water sample is pumped through capillary tubing and into a semi-permeable silicone membrane that is exposed to the vacuum inlet of a quadrupole mass spectrometer (QMS700, Pfeiffer). As the water flows through this membrane a fraction of the dissolved gases are extracted into the vacuum and directed towards the ion source of the mass spectrometer, after going through a cryotrap that removes water vapor and CO_2 . The ^{18}O -GOP method relies on the photosynthetic ^{18}O enrichment of the dissolved O_2 pool by the splitting of water, while the O_2/Ar -NOC relies on the change in the dissolved O_2 pool in relation to the dissolved Ar pool, with the latter being biologically inert. We calculate the gas concentrations of the samples in $\mu\text{mol L}^{-1}$ by measuring the m/z signal of a filtered ($0.2 \mu\text{m}$) seawater standard of known salinity that has been air-equilibrated overnight at a known temperature. Once in equilibrium with the atmosphere, we calculate the concentration of O_2 and Ar in the standard using the solubility equations of Garcia & Gordon (1992) and Hamme & Emerson (2004) respectively, to obtain a reference concentration for the measured m/z signal. The isotopic composition of dissolved O_2 in the standard was determined from the solubility fractionation reported by Kroopnick & Craig (1972). The standard was measured at the beginning and end of every MIMS session, as well as in between every 6 samples measured, to account for drifts in the signal (Ferrón et al., 2016).

Rate Calculations

Hourly rates of GOP (in $\mu\text{mol L}^{-1} \text{h}^{-1}$) are determined from the change in the O_2 isotopic composition during the incubation, following:

$$(3) \quad GOP = \frac{{}^{18}R(O_2)_{Light} - {}^{18}R(O_2)_{Zero}}{{}^{18}R(H_2O) - {}^{18}R(O_2)_{Zero}} \times [O_2]_{Zero} \times \frac{1}{t}$$

Where ${}^{18}R(O_2)$ is the isotope ratio of ${}^{18}O$ to ${}^{16}O$ of the oxygen molecules in the respective water sample (light or zero bottle), ${}^{18}R(H_2O)$ is the isotopic ratio of the water at the beginning of the incubation, and t is the incubation time in hours. The net oxygen change in the light and dark bottles, NOC (in $\mu\text{mol L}^{-1} \text{h}^{-1}$), is determined from the net change in O_2/Ar ratios (Bender et al., 1999), following:

$$(4) \quad NOC_{Bottle} = \left(\frac{(O_2/Ar)_{Bottle}}{(O_2/Ar)_{Zero}} - 1 \right) \times [O_2]_{Zero} \times \frac{1}{t}$$

Where we have the O_2/Ar ratio for the incubated bottle and zero bottle, as well as the initial oxygen concentration from the zero bottle. Since there is simultaneous oxygen production and consumption in the light incubation, respiration in the light can be determined from the difference between GOP and NOC from the light bottle (Eq. 5). Without a light source there is no photosynthesis, so NOC rates from Eq. 4 using the dark bottle are equivalent to daytime respiration in the dark (Eq. 6):

$$(5) \quad LR = GOP - NOC_{Light}$$

$$(6) \quad DR = NOC_{Dark}$$

A summary of the metabolic rates dataset created from applying these calculations is presented in Table 2.

Table 2: Summary of metabolic rates for each treatment, showing the mean (\pm standard deviation) and range over the course of the experiment (in $\mu\text{mol O}_2 \text{ L}^{-1} \text{ h}^{-1}$), as well as the ratios between the treatment means from the first and last day of sampling the PERIcosms (“Tf:Ti”: time-final to time-initial ratios).

Treatment	GOP			LR			DR			NOC		
	Mean \pm SD	Range	Tf:Ti	Mean \pm SD	Range	Tf:Ti	Mean \pm SD	Range	Tf:Ti	Mean \pm SD	Range	Tf:Ti
<i>C</i>	0.02 \pm 0.01	0.01 – 0.05	2.9	0.1 \pm 0.03	0.04 – 0.14	0.8	0.09 \pm 0.03	0.03 – 0.16	2.7	-0.06 \pm 0.03	-0.1 – 0.007	1.3
<i>F</i>	0.04 \pm 0.01	0.02 – 0.05	1.1	0.1 \pm 0.05	0.06 – 0.2	0.5	0.1 \pm 0.03	0.07 – 0.17	0.9	-0.07 \pm 0.05	-0.2 – -0.02	0.4
<i>N</i>	0.2 \pm 0.1	0.03 – 0.3	10.5	0.2 \pm 0.04	0.1 – 0.3	1.4	0.1 \pm 0.03	0.1 – 0.2	1.1	0.04 \pm 0.07	-0.1 – 0.1	-1
<i>NF</i>	0.2 \pm 0.1	0.03 – 0.4	13.6	0.2 \pm 0.03	0.1 – 0.2	1.1	0.1 \pm 0.02	0.1 – 0.2	0.8	0.05 \pm 0.1	-1.3 – 0.2	-1.4
<i>NP</i>	0.3 \pm 0.2	0.05 – 0.5	9.3	0.2 \pm 0.1	0.07 – 0.3	1.6	0.1 \pm 0.04	0.08 – 0.2	0.8	0.1 \pm 0.1	-0.1 – 0.2	-1.7
<i>NPF</i>	0.3 \pm 0.2	0.05 – 0.5	10.5	0.2 \pm 0.06	0.1 – 0.4	1.5	0.2 \pm 0.03	0.1 – 0.2	0.7	0.07 \pm 0.1	-0.2 – 0.2	-0.9
<i>P</i>	0.05 \pm 0.03	0.02 – 0.1	4.1	0.1 \pm 0.05	0.06 – 0.2	0.7	0.01 \pm 0.06	0.04 – 0.2	0.2	-0.05 \pm 0.07	-0.2 – 0.02	0.2
<i>PF</i>	0.06 \pm 0.04	0.02 – 0.14	7.4	0.1 \pm 0.05	0.05 – 0.2	1.0	0.07 \pm 0.04	0.02 – 0.2	0.6	-0.05 \pm 0.05	-0.2 – 0.002	0.2

Statistical Analysis

The statistical analysis was done through linear modeling in R (v3.5.1), with some Model II linear regressions and Pearson correlation statistics that were run in Python (v3.7.11). Linear mixed effects models were created using the function `lmer` from the `lme4` package (v1.1-29; Bates et al., 2015) with the formula:

$$(7) \text{ Response} \sim \text{AddedN} + \text{AddedP} + \text{AddedFe} + \text{AddedN}:\text{AddedP} + \text{AddedN}:\text{AddedFe} + \\ \text{AddedP}:\text{AddedFe} + \text{AddedN}:\text{AddedP}:\text{AddedFe} + (1|\text{Name}) + (1|\text{Date}) + \\ (1|\text{Date}:\text{AddedN}) + (1|\text{Date}:\text{AddedP}) + (1|\text{Date}:\text{AddedFe}) + (1|\text{Date}:\text{AddedN}:\text{AddedP}) + \\ (1|\text{Date}:\text{AddedN}:\text{AddedFe}) + (1|\text{Date}:\text{AddedP}:\text{AddedFe}) + \\ (1|\text{Date}:\text{AddedN}:\text{AddedP}:\text{AddedFe})$$

Where the right-hand side of the tilde has the predictor variables, and the left-hand side the response variables, meaning that the model would test for the effect of the predictor variables on the response data. In the equation, “Response” signifies the values measured during PERI-FIX (e.g., rates, concentrations, ratios); the three “*Added*” terms are Boolean labels of whether a treatment received a certain nutrient (e.g., “*AddedN*” is “*True*” for treatments N, NP, NF, and NPF; “*False*” for all other treatments), with the interaction between the different nutrients represented with colons (e.g., “*AddedN:AddedP:AddedFe*”); “(1|Date)” the random effect for the variation in the response over time that is shared across nutrient treatments; “(1|Tank)” is the random effect accounting for repeated measures of the experimental units (i.e., each of the 24 tanks); the “(1|Date:Added)” terms are time:treatment random effects that quantify whether the effect of a nutrient treatment or an interaction between nutrient treatments changes over time. For more information on fitting linear mixed models with the `lmer` function, see Bates et al. (2015). Fixed effects of nutrient addition were tested with approximate F-tests with the package `lmerTest` (v3.1-3; Kuznetsova et al., 2017) and the random

effect's interaction between nutrient addition with time were tested with marginal Chi-squared likelihood ratio tests.

Results

On collection day, August 9th, 2021, incubations for metabolic rates and complementary assessments of the seawater in the collection totes were performed, with the results presented in Table 3.

Table 3: Mean values (\pm SD; n = 3) for metabolic rates ($\mu\text{mol O}_2 \text{ L}^{-1} \text{ h}^{-1}$), chlorophyll ($\mu\text{g L}^{-1}$), and inorganic nutrients ($\mu\text{mol L}^{-1}$) of the unfiltered seawater in the totes on collection day (August 9th, 2021). See appendix for more information on complementary measurements such as: Nitrate + Nitrite (N+N), Soluble Reactive Phosphate (SRP), ammonium (NH_4^+), and chlorophyll (Chl).

GOP	LR	DR	NOC	Chl
0.02 \pm 0.02	0.03 \pm 0.03	0.02 \pm 0.02	0.00 \pm 0.02	0.16 \pm 0.0
N+N	SRP	Si	NH₄⁺	
0.035 \pm 0.016	0.066 \pm 0.006	1.3 \pm 0.1	132.5 \pm 20.6	

Gross Oxygen Production

The first clear response in GOP was the difference in rates between treatments with and without N added (Fig. 1), with our statistical results showing a significant effect from N addition on GOP (Table 4). All tanks with N added had a significant increase in productivity two days from their first nutrient addition. After the first initial increase in GOP there was a decrease within the first week, possibly because nutrient additions were halted on August 13th and 14th. Once nutrient additions resumed there was constant increase in GOP rates for the following three weeks, culminating in final rates 9 to 14-fold larger than at the start of the experiment. GOP in the treatments with N added were significantly higher than in all the treatments without N (Table 4). Treatments NP and NPF reached the highest rates overall—around a 20-fold increase in some tanks by the end of the experiment (Fig. 1A, Table 4). For

the treatments without N added, productivity in the P and PF treatments responded similarly to N addition but GOP increased by a much smaller magnitude (Fig. 2), until they showed a slow but steady increase from August 23rd onwards which, while still relatively low compared to the treatments with added N, culminated in a 4- to 5-fold increase in GOP. Productivity remained relatively constant in the C and F treatments throughout the experiment, and the addition of Fe showed no significant effect (Table 4).

When contrasting our GOP results with complementary measurements (see Appendix), there was a very similar response of chlorophyll (Chl) concentrations to nutrient additions (Fig. A1) and significant positive correlation between GOP and Chl ($R^2 = 0.827$, $p < 0.01$; Fig. A2), indicating the possibility that variations in productivity were at least partly driven by changes in phytoplankton biomass. When the GOP data is normalized to Chl, the ratio varies within the range of 0.15 and 0.6 ($\mu\text{mol O}_2 (\mu\text{g Chl})^{-1} \text{h}^{-1}$) with no clear trends for the different treatments (Fig. A3), although the linear mixed models still show a significant increase in the GOP to Chl ratio in response to N addition (Table 4).

Metabolic Rates in $\mu\text{mol O}_2 \text{ L}^{-1} \text{ h}^{-1}$

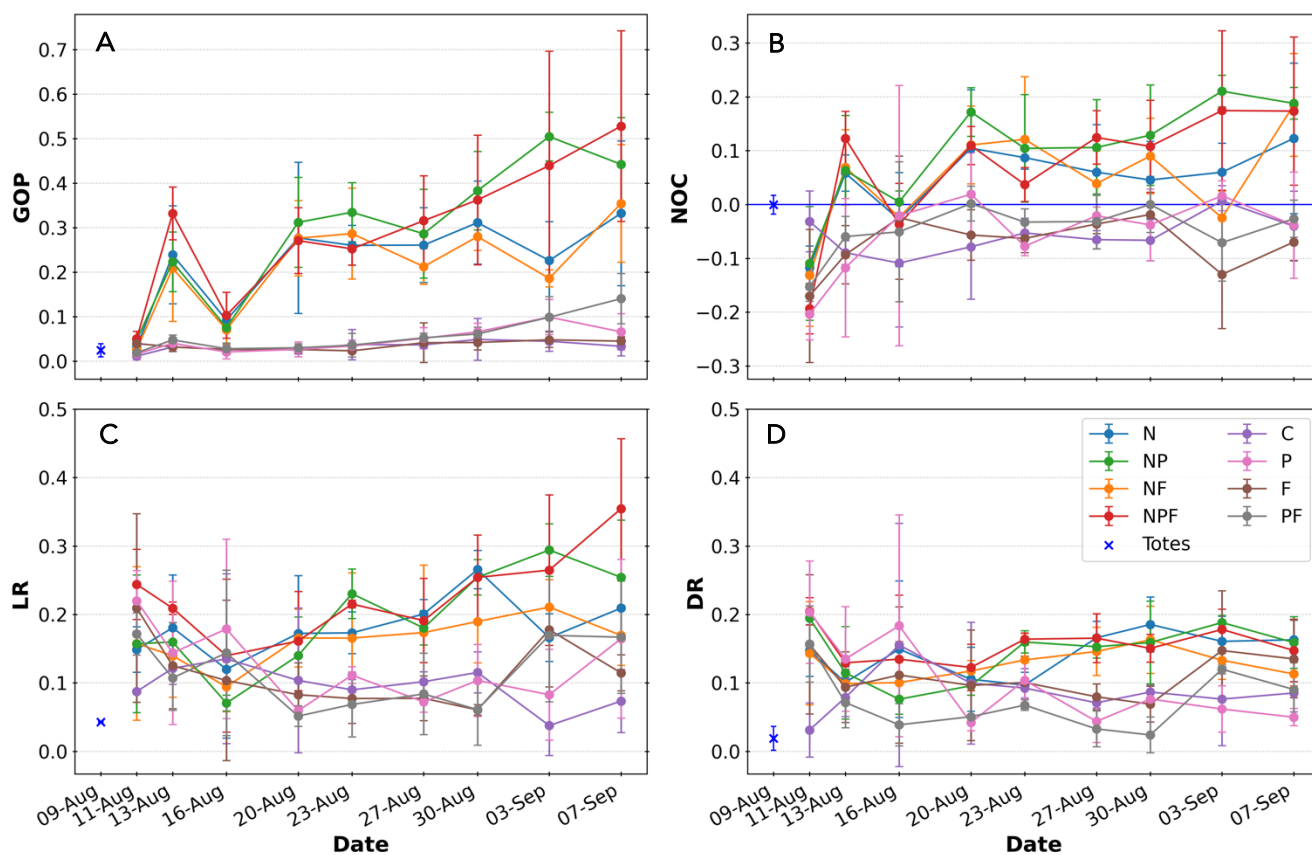


Figure 1: Plot of the daily means of each treatment, with standard deviation as error bars ($n = 3$ tanks per treatment), for: **A)** Gross Oxygen Production; **B)** Net Oxygen Change; **C)** Light Respiration, and **D)** Dark Respiration. **All)** All values are in $\mu\text{mol O}_2 \text{ L}^{-1} \text{ h}^{-1}$. The mean values (\pm standard deviation) for the totes on offshore collection date are also included (Table 3) as a blue cross. For NOC, a blue line at $y = 0$ is included for reference, with positive and negative values indicating net autotrophic and heterotrophic conditions throughout the incubation, respectively.

Daytime Light and Dark Respiration

LR rates during the experiment were all higher than those measured on collection day and, similarly to GOP, there was a significant response from LR to N addition, although with a reduced dynamic range (Fig. 1C; Table 4). LR had a sharp increase in all treatments between the collection totes' measurements and the first sampling day, which then gradually decreased during the first week of the experiment. After the first week there is a gradual increase in rates for tanks that were provided N, with once again the NP and NPF treatments showing the highest rates, much like GOP, without being significantly different from other treatments with N (Table 4). For the treatments without N added, the P, F, and PF treatments were higher both at the beginning and the end of the experiment, with relatively

constant, lower rates during the middle of the experiment, yet there was no statistically significant effect in LR from P or Fe addition (Table 4).

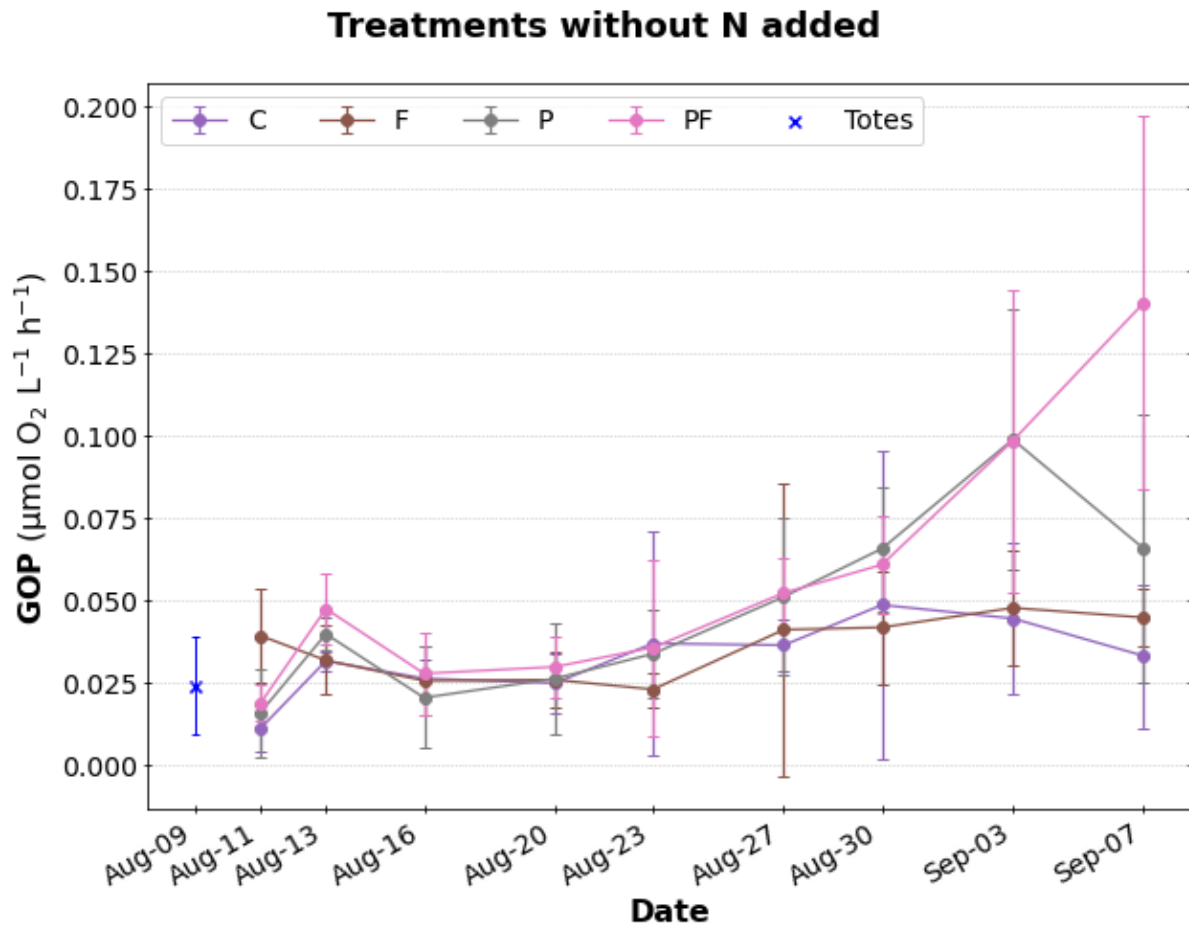


Figure 2: Close-up of the evolution of GOP (mean \pm standard deviation) for the treatments that were not provided with inorganic nitrogen. The mean values (\pm standard deviation) for the totes on collection day (Table 3) are also included as a blue cross.

DR rates were also higher inside the PERICosms compared to the collection day rates, with a sharp decrease in the first few days that led to a small but significant separation between treatments with and without N provided, illustrating a significant effect of N addition on DR increase, but with an even further reduced dynamic range than LR (Fig. 1D; Table 4). The two respiration estimates correlate well (Fig. 3B), but the slope of 1.6 shows that the Model II linear regression estimates LR to be 160% of DR on average, while the ratio of mean LR and mean DR was 1.3 for the entire experiment. This indicates a more conservative estimate of LR being 30% greater than DR, while also illustrating a higher

variability in LR. There was no significant effect of nutrient addition on the LR:DR ratio, yet there was a significant response in the difference between LR and DR to N addition (Figs. 4A & 4C; Table 4). When contrasting the daytime light to dark respiration ratio and daytime light and dark respiration difference with GOP, both estimates correlate significantly with GOP for the treatments provided with N (Figs. 4B and 4D)

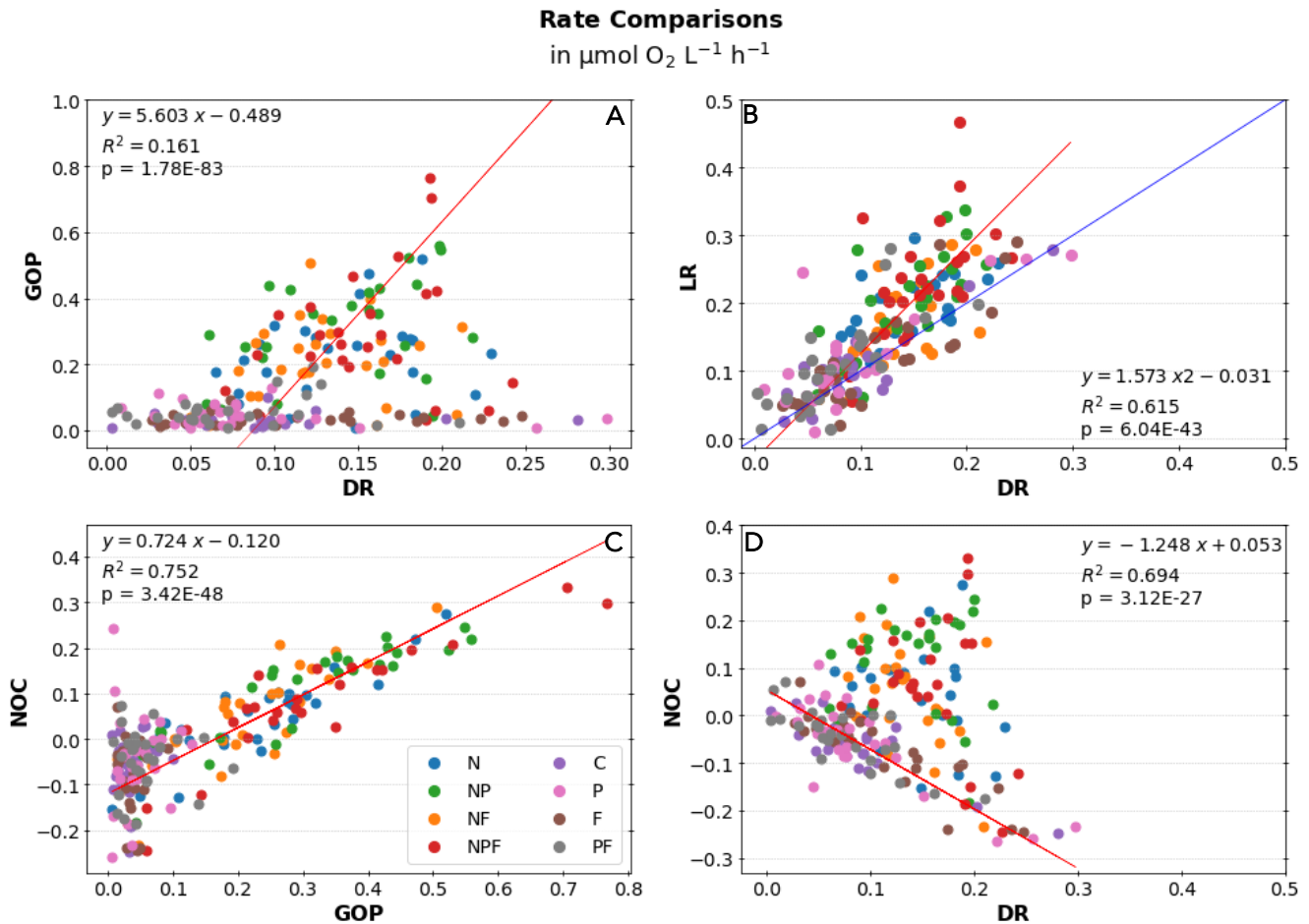


Figure 3: Plot of the correlations between metabolic rates (in $\mu\text{mol O}_2 \text{ L}^{-1} \text{ h}^{-1}$), with Model II linear regression fit in red, the regression equation, and Pearson's correlation R^2 and p values. **A)** Correlation between Dark Respiration and Gross Oxygen Production (regression fit includes all points regardless of treatment), **B)** Correlation between Light Respiration and Dark Respiration (regression fit includes all points; 1:1 line is shown in blue), **C)** Correlation between Gross Oxygen Production and Net Oxygen Change (regression fit for treatments with N added), and **D)** Correlation between Dark Respiration and Net Oxygen Change (regression fit for treatments without N added).

Respiration Comparisons

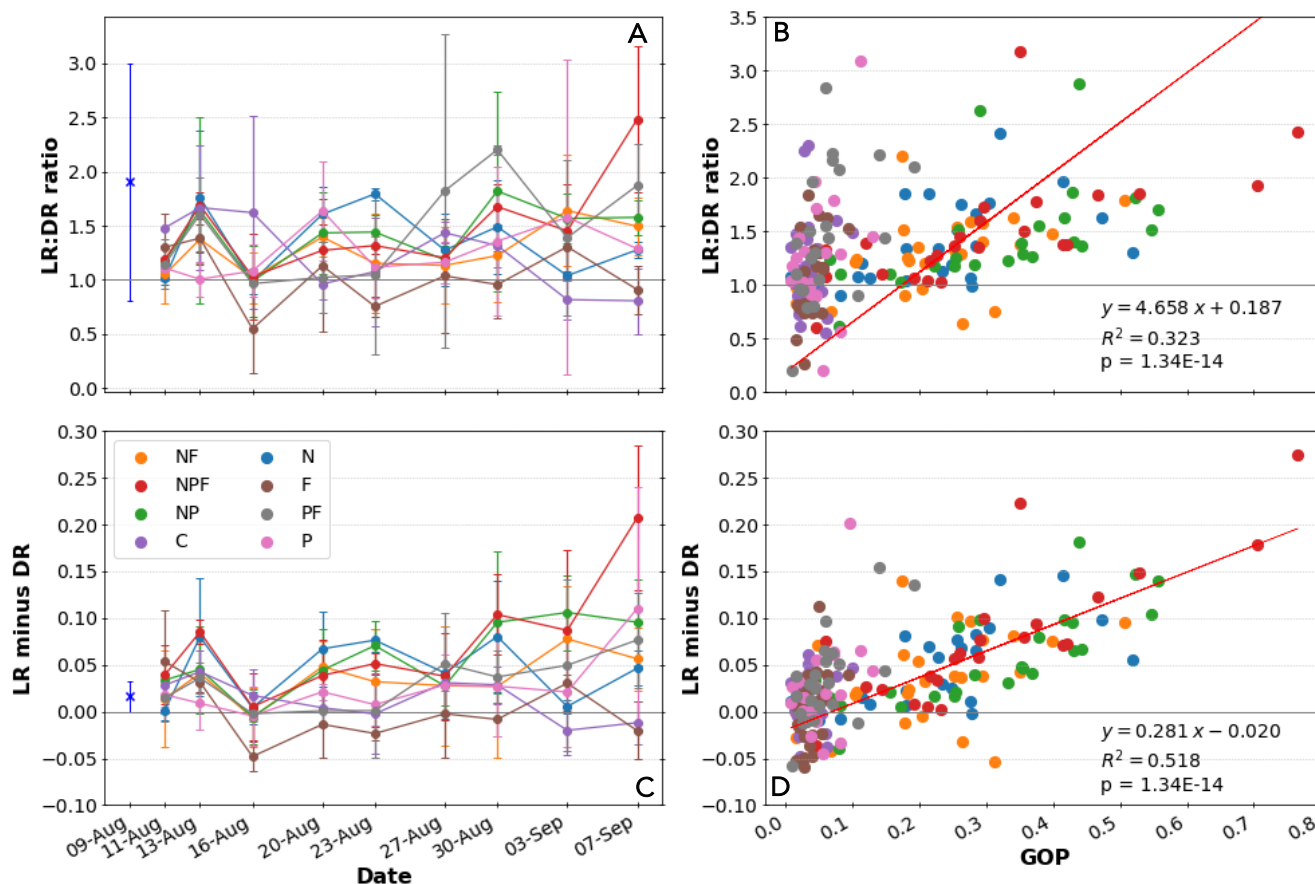


Figure 4: Plots of comparisons between LR and DR. **A)** Evolution of the daily means of the daytime light to dark respiration ratio, **B)** Correlation of LR:DR with GOP, **C)** Evolution of the mean difference between daytime light and dark respiration, in $\mu\text{mol O}_2 \text{ L}^{-1} \text{ h}^{-1}$, for each treatment. **D)** Correlation of the daytime light and dark respiration difference and GOP. **A & C)** Standard deviation is included as error bars ($n = 3$ tanks per treatment). The mean values (\pm standard deviation) for the totes on collection day are also included (Table 3) as a blue cross. **B & D)** Red lines are Model II linear regression fits, with the regression equation and Pearson's correlation R^2 and p values. The GOP axis is in units of $\mu\text{mol O}_2 \text{ L}^{-1} \text{ h}^{-1}$. A gray line at $y = 0$ is included for reference on all panels.

Net Oxygen Change in the light

The collection day measurements showed NOC values near metabolic balance, yet on the first sampling day all treatments showed net heterotrophy over the incubation period (Fig. 1B), due to an increase in respiration (Figs. 1C & 1D). In similar fashion to GOP and LR, there is again a separation in NOC rates between treatments with and without N provided, with the former group increasing NOC and transitioning into net autotrophic conditions (for the 6-hour incubations), remaining there from the twelfth day of the experiment onwards. NOC in treatments with N spikes also track the boom and crash that occurred in the first week of the experiment in GOP. In treatments spiked with N, changes in NOC

tracked changes in GOP, whereas in treatments without N added NOC tracked changes in DR (Figs. 4C & 4D). When hourly NOC rates are extrapolated to obtain NCP for 24-hour periods through Eq. 8, the results show net heterotrophic conditions for most of the experiment, until the last sampling day when most tanks with N added reached net autotrophic values (Fig. 5).

$$(8) \quad NCP = (NOC_{Light} * 13) - (DR * 11)$$

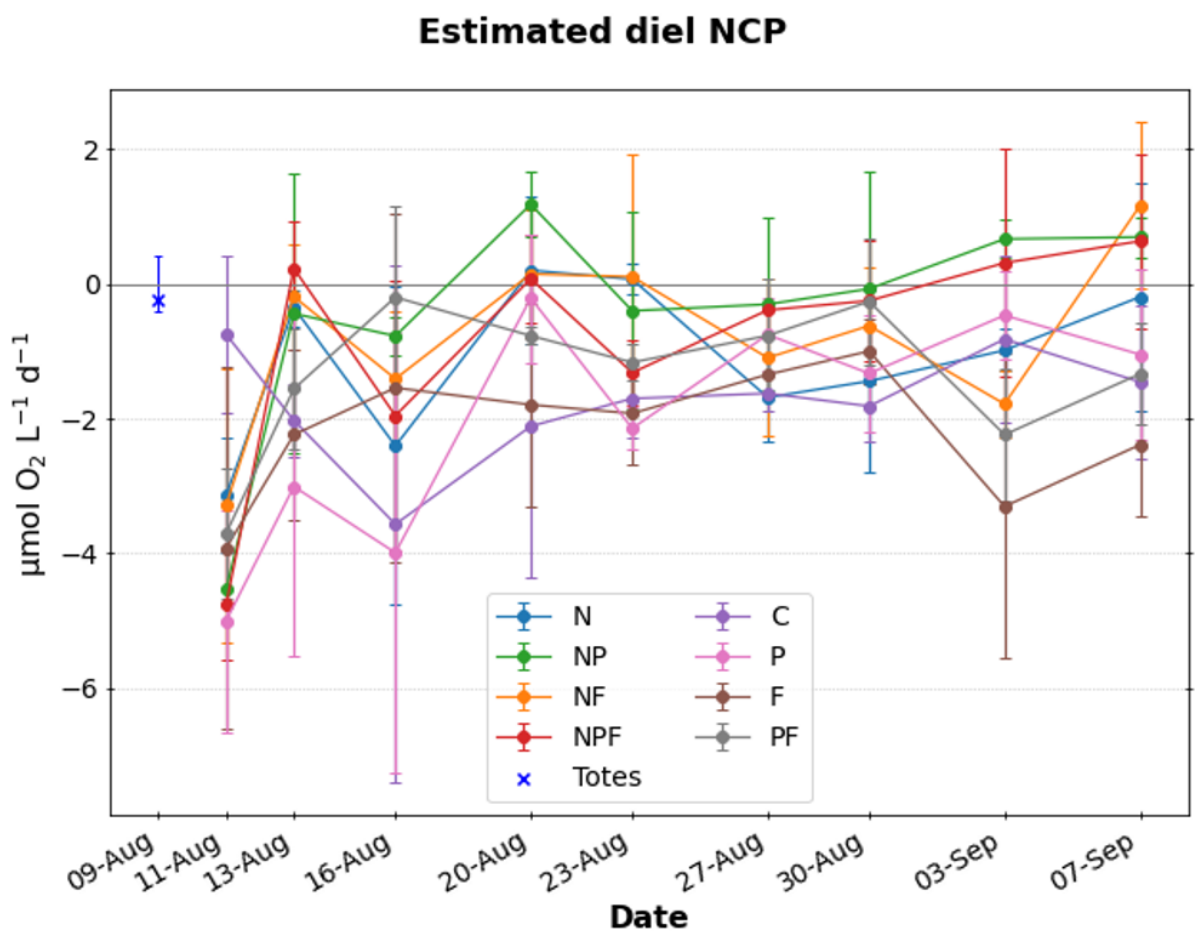


Figure 5: Evolution of diel NCP (mean \pm standard deviation; $n = 3$ tanks per treatment) in $\mu\text{mol O}_2 \text{ L}^{-1} \text{ d}^{-1}$, for each treatment during PERI-FIX, estimated using Eq. 8.

Table 4: Statistical results from fitted linear mixed models. Data includes p-values and denominator degrees of freedom for approximate F-test for the significance of the response to nutrient addition, as well as p-values for Chi squared tests for the significance of the interaction between nutrient addition and time. All numerator degrees of freedom for approximate F-tests and degrees of freedom for Chi sq. tests were equal to one. An empty cell for the Chi sq. test signifies an estimated variance of 0 for the random effect (time). Significant p-values ($p < 0.05$) are highlighted in bold text. Significant F-test p-values denote an effect from the predictors on the response, while significant Chi sq. test p-values denote a significant change in variance with time.

Response	Predictor	F-value (df)	F-test p-value	Chi sq value	Chi sq. p-value	Response	Predictor	F-value (df)	F-test p-value	Chi sq. value	Chi sq. p-value
GOP	N	75.6 (10)	4.11E-6	7.9	0.005	NOC	N	30 (9)	0.0003	11.7	0.0006
	P	6.1 (14)	0.03	0.2	0.63		P	2.9 (10)	0.12	1.5	0.22
	Fe	0.6 (12)	0.46	0.6	1		Fe	0.3 (10)	0.6	0.3	0.61
	N:P	0.02 (13)	0.9		0.47		N:P	0.5 (16)	0.48		
	N:Fe	1.4 (16)	0.26				N:Fe	0.2 (16)	0.67		
	P:Fe	0.2 (16)	0.7				P:Fe	0.1 (16)	0.73		
	N:P:Fe	0 (16)	1				N:P:Fe	1.1 (16)	0.31		
LR	N	15.6 (20)	0.0008	0.1	0.72	DR	N	16.9 (24)	0.0004		
	P	1.5 (13)	0.25	0.06	0.8		P	0.2 (19)	0.69	0.5	0.49
	Fe	0.03 (20)	0.88				Fe	0.001 (22)	0.97		
	N:P	0.06 (16)	0.81				N:P	1.7 (15)	0.22	1	0.32
	N:Fe	0.004 (20)	0.96	7.6	0.006		N:Fe	0.02 (22)	0.9	5.1	0.024
	P:Fe	0.02 (16)	0.88	0	1		P:Fe	0.9 (16)	0.37		
	N:P:Fe	1.9 (16)	0.19				N:P:Fe	3 (16)	0.1		
LR to DR ratio	N	0.5 (13)	0.5	0.03	0.87	LR minus DR	N	10.7 (14)	0.006	2.4	0.12
	P	3.2 (13)	0.09				P	2.5 (15)	0.13	3.4	0.07
	Fe	0.3 (14)	0.61				Fe	0.0004 (13)	0.99	0.01	0.92
	N:P	1.8 (13)	0.2	0.2	0.24		N:P	0.1 (16)	0.75		
	N:Fe	0.4 (14)	0.54				N:Fe	0.1 (16)	0.71	0	1
	P:Fe	1.2 (14)	0.3				P:Fe	1.4 (13)	0.25	0.3	0.59
	N:P:Fe	0.6 (14)	0.44				N:P:Fe	0.09 (16)	0.77		
GOP to Chl ratio	N	13.8 (6)	0.011	0	1	Chl	N	68 (12)	3.45E-6	7.7	0.005
	P	4.2 (16)	0.057				P	1.7 (15)	0.21	1.4	0.24
	Fe	0.1 (7)	0.75	1.02	0.31		Fe	0.3 (15)	0.61	1.8	0.18
	N:P	0.6 (16)	0.45				N:P	0.03 (13)	0.87	0.02	0.9
	N:Fe	0.03 (16)	0.87	0	1		N:Fe	2.5 (16)	0.13		
	P:Fe	0.02 (16)	0.89				P:Fe	0.05 (16)	0.83		
	N:P:Fe	1 (16)	0.33				N:P:Fe	0.2 (16)	0.67		

Discussion

Effects of Nitrogen Supply

The most noticeable effect on phytoplankton biomass and productivity came from the supply of N to the PERIcosms. The addition of inorganic N resulted in a rapid increase in chlorophyll concentrations and GOP two days after the start of the experiment and supported a shift in metabolic state from net heterotrophy to net autotrophy over the incubation period (Figs. A1, 1A & 1B). This initial boost went away on August 16th, after nutrient additions were halted for August 13th and 14th, but both GOP and chlorophyll concentration increased again quickly as soon as the nutrient additions were resumed. The rapid response of phytoplankton to the addition of inorganic N is consistent with previous manipulation experiments in the NPSG (Böttjer-Wilson, 2021; Mahaffey et al., 2012; McAndrew et al., 2007) that showed a quick response (<1 week) in biomass and carbon fixation rates by the surface microbial community to the addition of nutrients or nutrient-rich deep sea water (DSW). Our data also suggests that when N was added, the supplementary addition Fe did not have a significant effect on GOP, indicating that this nutrient did not become limiting in the treatments with N spikes (Table 4).

Mahaffey et al. (2012) conducted paired incubations of DSW and nitrate additions (~2 μ M nitrate added for each), seeing an increase of chlorophyll and carbon fixation of up to 18- and 22-fold, respectively, during the summer, that was similar in magnitude and timing (2 days) for both the DSW and nitrate only additions, indicating no noticeable effect for the supplementary addition of phosphate or iron in DSW. However, that was not the case during the winter, when DSW had a larger effect than lone nitrate addition. Böttjer-Wilson et al. (2021) conducted nutrient additions in paired mesocosm and microcosm experiments, focusing on the manipulation of P supply by providing a suite of nutrients lacking inorganic P to their “P⁻” treatment and providing the same nutrients but with inorganic phosphate to their “P⁺” treatments. This study reported similar maxima in productivity and chlorophyll

for both P+ and P– treatments, but there was a faster response (4 days) in both P+ microcosms and mesocosm compared to their P– counterparts (6 days).

The quick response of phytoplankton to the addition of inorganic N is somewhat expected, given the low concentration of nitrate (~40 nM) in the water collected for this experiment, and the low nitrate to phosphate ratio of ~3, nearly 5 times lower than Redfield. However, at the nearby HOT time-series site, Station ALOHA, where surface waters are chronically depleted in inorganic N (typically < 10 nM), there are occasional spikes in N surface inventories—typically in the winter—with no accompanying increase in productivity, suggesting an alternate interaction between nutrient availability and productivity that is not well understood (Karl et al., 2021). Related to this, Mahaffey et al. (2012) showed that the timing and magnitude of the phytoplankton response to changes in nutrient supply is seasonal, being faster and stronger in the summer compared to winter. These discrete responses suggest a relationship to the decoupling of N and P in the NPSG, where nitrogen fixation and the selective retention of P by organisms could exacerbate P-limitation, and thus affect the response to a nutrient pulse (Karl et al., 2001b).

The phosphate concentrations for all treatments with N addition remained very low (<40 nM) after the 16th of August regardless of whether P was added or not (Fig. A4)—values well below the threshold for P limitation estimated by Letelier et al. (2019) for the NPSG (~50-60 nmol kg⁻¹). Inorganic N and P net uptakes were estimated for the length of the experiment as the difference between the expected concentration of the given nutrient (based on the initial concentration and the total amount added) minus its final concentration. The estimated nitrate to phosphate uptake ratios are substantially different between treatments with N added that were also provided with P (N:P ~ 11) and without P spikes (N:P ~ 40). The values well above Redfield ratio for the treatments with N but no supplemental P imply that the organisms in these treatments must be securing their P elsewhere. In fact, Mahaffey et al. (2014)

showed that alkaline phosphatase activity (APA), an enzyme which allows organisms to hydrolyze phosphate esters in the DOP pool, was higher in subtropical waters with $<30\text{nM}$ concentrations of phosphate, as well as being induced and repressed by the addition of N and P, respectively. Access to P from the dissolved organic pool could therefore explain our large, estimated N:P uptake ratios and the similarity of the phytoplankton response in all treatments with N spikes (with or without P added). The ratio below Redfield in the tanks with both N and P could also be related to the storing of “luxury” P (i.e., excess in relation to Redfield) by the microbial community (Karl, 2000).

The increase in primary productivity and biomass after August 16th coincided with a sharp decrease in silicate concentrations, presumably due to uptake by diatoms, highlighting their role on the community response to N supply (Fig, A4C). Net uptake rates for silica were also calculated similar to N and P, but from the beginning of the experiment until August 21st, when concentrations of silica were lowest. These Si:N uptake ratios were ~ 0.6 for treatments spiked with N, near the lower end of the 0.8 ratio established by Brzezinski (1985), suggesting a significant consumption of N by diatoms. The shift of the microbial community structure towards a diatom-dominated composition after a nutrient pulse has been theorized and observed in other manipulation experiments. The transition from nutrient depleted to nutrient replete conditions in these experiments typically carry shifts in microbial community composition, including an increased size of organisms and a prevalence of diatoms (Alexander et al., 2015; Böttjer-Wilson et al., 2021; Mahaffey et al., 2012; McAndrew et al., 2007). Additionally, Karl & Letelier (2008) proposed a two-stage bloom could be created in the NPSG by mixing DSW (with low inorganic N:P) with the oft stratified surface waters: the first stage would be a diatom bloom that would consume all the inorganic nitrogen, and once the inorganic nitrogen is depleted but there are still P and Fe available, the second stage would be a diazotroph bloom. The first stage bloom is consistent with our results as well as the manipulation experiments mentioned (Alexander et al., 2015; Mahaffey et al.,

2012, McAndrew et al., 2007). The very low phosphate concentrations in our experimental setting could preclude the development of a N_2 fixation bloom in the treatments with N additions.

Our results for the addition of N also show a clear shift in metabolic state from net heterotrophy to net autotrophy during incubations. The slope of the correlation between GOP and respiration implies that inorganic N addition effected a larger increase in GOP than LR or DR (Fig. 3A), resulting in an increase of NOC with the supply of inorganic N. In the field, this could imply increasing the C export potential following an inorganic N supply event, particularly given the importance of diatoms in driving the increase in biomass. McAndrew et al. (2007) showed increased NCP after the addition of DSW in manipulation experiments at Station ALOHA. This rapid increase in NOC supports the hypothesis that sporadic short-lived nutrient injections could support the net autotrophic state of the NPSG and explain short-term O_2 variability (Karl et al., 2003). However, under our experimental conditions the extrapolated diel NCP values from Eq. 8 only become positive at the end of the experiment (Fig, 5), due to the significant contribution of DR to NCP, possibly because of the highly heterotrophic conditions at the beginning of the experiment which do not seem to represent natural conditions based on the time-zero rates.

Effects of Phosphorus and Iron Supply

Being able to access the hefty dissolved N_2 pool as a source of inorganic N should be able to alleviate the nitrogen limitation evident from the microbial response in the treatments where N was supplied. N limitation to primary productivity has been suggested to be a prerequisite for inducing nitrogen fixation, as nitrogen additions have been shown to repress nitrogen fixation regardless of location (Mills et al., 2004). However, recent studies have shown nitrogen fixation activity by organisms that still had nitrate available (Meyer et al., 2016; Turk-Kubo et al., 2018), indicating an increased role for other limiting nutrients such as phosphate and iron.

Our results do not show an effect of Fe supply in metabolic rates, as the F treatment was most similar to the control, indicating that Fe supply did not enhance N₂ fixation. This is despite nitrogen fixation thought to be primarily limited by iron, as iron is a major cofactor in the nitrogenase enzyme (Falkowski, 1997). Conceptual frameworks rooted in resource ratio theory (Schade et al., 2005; Tilman et al., 1982) have shown that the global biogeography of diazotrophs is mainly constrained by the Fe:N supply ratio, with a secondary role for the P:N supply ratio (Dutkiewicz et al., 2012; Ward et al., 2013). The role of iron in limiting N₂ fixation has also been shown in previous manipulation experiments in the North Atlantic seeking to induce nitrogen fixation through the addition of P and/or Fe (Meyer et al., 2016; Mills et al., 2004; Mills & Arrigo, 2010). The interaction between P and Fe in limiting N₂ fixation is complex. Letelier et al. (2019) proposed that long-term oscillations between P-sufficiency and P-limitation in the eastern NPSG occur through climate patterns of Fe-rich dust delivery from Asia. These authors suggested that aeolic iron inputs would further N₂ fixation, depleting the P pool below a hypothetical P-limitation threshold of 50–60nM of inorganic P for the mixed layer microbial community. The role of phosphorus in nitrogen fixation is further exemplified in the NPSG two-stage bloom hypothesis, as the second stage relies on the first stage not only to deplete the nitrate pool, but to leave enough residual phosphate to support the development of its diazotrophic bloom (Karl & Letelier, 2008) and is applicable beyond the North Pacific (Weber & Deutsch, 2010).

During the PERI-FIX experiment, the effects of P supply on primary productivity were muted compared to N supply, but there was still an initial response on August 13th much like the initial bloom in the tanks spiked with N (Fig. 2). After August 20th, there was a noticeable increase in GOP for the P and PF treatments that led to final rates more than two- and four-fold, respectively, than the control treatment, hypothetically coming from N₂ fixation-supported primary production. Furthering this thought, if we extrapolate cumulative GOP for the 30 days of the experiment, and calculate excess

oxygen production in the P and PF tanks relative to the control, we estimate that this “excess” in production needs to be supported by approximately $0.08 \mu\text{mol N L}^{-1}$ for P and $0.25 \mu\text{mol N L}^{-1}$ for PF, using a Redfield $\text{O}_2\text{:N}$ stoichiometry of roughly 144:16. If it is assumed that this deficit in N needed to support the enhanced primary production is entirely supplied by N_2 fixation, N_2 -fixation rates for the experiment would be on average ~ 3 and $\sim 8 \text{ nmol N L}^{-1} \text{ d}^{-1}$ for P and PF, respectively, which are values comparable to published surface N_2 fixation rates from St. ALOHA (Böttjer et al., 2017; Zehr et al., 2007). Experimentally, the sole addition of dissolved inorganic P and/or dissolved organic P within manipulation experiments in the NPSG has been shown to have an effect on both carbon and nitrogen fixation (Grabowski et al., 2008; Watkins-Brandt et al., 2011; White et al., 2010), as long as the background inorganic P concentrations are below 40 nM (Grabowski et al., 2008; Gradoville et al., 2014). The initial inorganic P concentration in the water used for this experiment (67 nM; Table 3) was very close to the hypothetical P-limitation threshold of 50–60 nM proposed by Letelier et al. (2019). Therefore, presumably the lack of excess inorganic P precluded the diazotrophs from thriving in the single Fe treatment.

Patterns in Light and Dark Respiration

Studies focusing on aquatic respiration have historically lagged behind those of aquatic primary productivity, with measurements of respiration in the ocean only accounting for 1% of the global measurements of primary productivity by the ^{14}C method (Robinson & Williams, 2005). Because of this lack of attention, del Giorgio & Williams (2005) considered respiration as the largest gap in understanding the global carbon cycle, highlighting surface open ocean respiration rates as the most uncertain component of global respiration estimates. Most of these respiration measurements rely on the use of “light” and “dark” bottles to separate oxygen production (Eq. 1) from oxygen consumption (Eq. 2), with the oxygen change in the “dark” bottle equating respiration and extrapolated to diel rates (Bender et al., 1987). However, some studies have shown that respiration is not constant during the

nighttime in cultures and lakes (Mantikci et al., 2019; Markager et al., 1992; Markager & Sand-Jensen, 1989), and others that the rates of respiration measured in the light could be significantly higher than those in the dark for cultures, lakes, and even in high-Arctic waters (Bender et al., 1987; Grande et al., 1989; Kana, 1990; Lewitus & Kana, 1995; Mesa et al., 2017; Pringault et al., 2007).

In this experiment we measured respiration during daytime under both light and dark conditions. The significant effect of inorganic N addition on both estimates of respiration (Table 4) demonstrates that supplying the nutrient limiting primary production to the PERIcosms increased respiration rates as well, though to a lesser magnitude than productivity as evidenced by the increasing NOC in the treatments with N added. This result is consistent with literature on the relationship between photosynthesis and respiration (Robinson & Williams, 2005). No significant effect on respiration from P or Fe addition was present (Table 4). Values for LR and DR correlate well, but the regression's slope of ~ 1.6 in Fig. 3B indicates that LR was on average 160% of DR during the experiment, while the mean ratio between LR and DR was 1.3 for the entire experiment, showing enhanced daytime respiration rates in the light for PERI-FIX. In experiments that have measured respiration in both light and dark conditions in microbial cultures, lakes, the Arabian sea, and both Arctic and Antarctic waters, the majority have found LR to be 0.5 to 10 times greater than DR rates (Bender et al., 1987; Dickson et al., 2001; Dickson & Orchardo, 2001; Grande et al., 1989; Kana, 1990; Lancelot & Mathot, 1985; Lewitus & Kana, 1995; Mesa et al., 2017; Pringault et al., 2007; Robinson et al., 2009). In fact, Mesa et al. (2017) saw an increasing difference between LR and DR with increasing ^{18}O -GOP values, much like the relationship we see in Fig. 4D. This detectable increase in O_2 consumption in the light could be due to enhanced mitochondrial respiration, chlororespiration, photorespiration, and/or the Mehler reaction (Bender et al., 1999). Lewitus and Kana (1995) proposed that chlororespiration was only induced at low-light intensities in energy-rich cells, and Mehler reaction activity increased in high-light, energy-limited organisms. These assessments would theoretically exclude our treatments with N

from the effects of chlororespiration (irradiance $>40 \mu\text{mol m}^{-2} \text{s}^{-1}$), and the Mehler reaction, as they are energy-rich treatments. In addition, the contribution of photorespiration under balanced growth irradiance (i.e., below saturating) is expected to only be modest (Lewitus & Kana, 1995).

Research has shown that photosynthesis enhances phytoplankton dark respiration as accumulated photosynthetic products become substrates for oxidation (Falkowski et al., 1985; Lancelot & Mathot, 1985; Mantikci et al., 2017). Through nutrient manipulation experiments, Roberts & Howarth (2006) also showed that community respiration increases with increasing nutrient availability, but also that it increases the proportion of community respiration phytoplankton are responsible for. This heightened role for phytoplankton relates to the exponential decrease of respiration rates that has been seen in cultures in dark conditions (Falkowski et al., 1985), as well as nighttime respiration rates in lakes being higher when measured after sunset than when measured before sunrise (Markager et al., 1992; Markager & Sand-Jensen, 1989). As the respiratory substrate is depleted throughout the nighttime, communities are known to reach a near-constant respiration rate by the end of the night (Markager et al., 1992). Because of this, our estimates of DR are potentially an underestimation of nighttime respiration, as the incubations were undertaken during daytime after a full night of darkness respiring the previous day's photosynthetic products. The difference in respiratory substrate pools between the samples incubated in the light and the dark could explain the differences observed in LR and DR, with respiration enhanced in the light by phytoplankton primary production.

The differences observed between LR and DR, particularly noticeable at high productivity, and indicating diel variability in respiration rates, have significant implications for effectively constraining the oceanic carbon cycle. Pringault et al. (2007) emphasized the need for properly accounting for daytime respiration, with their results showing a possible underestimation of GPP of up to 650% when only using respiration in the dark for coastal seawater samples. An ideal estimate of respiration for

accurate NCP determination in aquatic ecosystems would entail a diel incubation that could encapsulate both the effects of light on respiration and photosynthesis, as well as the consumption of photosynthates and exponential decrease in respiration rates during nighttime. Ancillary measurements for determination of photorespiration and Mehler reaction would be necessary as well to increase the accuracy of rates obtained by the ^{18}O -GOP method.

Conclusions

The results from monitoring the metabolic response in the enclosures to different nutrient addition regimes yielded three highlights. First, N was the main nutrient limiting the microbial community's primary production, with the supply of inorganic nitrogen effecting a 9 to 14-fold increase in productivity, as well as supporting a shift in metabolic state from net heterotrophy to net autotrophy during the incubation windows. The phosphate concentrations were driven below 40nM in all tanks provided with inorganic N, indicating that the microbial community is accessing other sources of P in the treatments with no supplemental inorganic P added, such as the dissolved organic P pool. Second, the supply of P effected a 4 to 7-fold increase in productivity in tanks where N was not provided, suggesting a possible enhancement through N₂-fixation. Yet, no effect on metabolic rates was observed for the single addition of Fe for the duration of the experiment, as it was most similar to the control tanks, possibly because of P-limitation to the diazotrophic community. Lastly, LR rates were estimated to be on average 1.3 times DR rates, with the difference between the two increasing with productivity. The difference between both estimates of respiration could be potentially explained by the increase in photosynthetic substrates available for respiration in the light samples, indicating that rates of community respiration vary throughout the day. This highlights the importance of properly accounting for these diel variations in respiration when constraining the carbon cycle.

References

- Alexander, H., Rouco, M., Haley, S. T., Wilson, S. T., Karl, D. M., & Dyhrman, S. T. (2015). Functional group-specific traits drive phytoplankton dynamics in the oligotrophic ocean. *Proceedings of the National Academy of Sciences of the United States of America*, 112(44), E5972–E5979. <https://doi.org/10.1073/pnas.1518165112>
- Antoine, D., André, J.-M., & Morel, A. (1996). Oceanic primary production: 2. Estimation at global scale from satellite (Coastal Zone Color Scanner) chlorophyll. *Global Biogeochemical Cycles*, 10(1), 57–69. <https://doi.org/10.1029/95GB02832>
- Bar-On, Y. M., Phillips, R., & Milo, R. (2018). The biomass distribution on Earth. *Proceedings of the National Academy of Sciences of the United States of America*, 115(25), 6506–6511. <https://doi.org/10.1073/pnas.1711842115>
- Bates, D., Mächler, M., Bolker, B., & Walker, S. (2015). Fitting linear mixed-effects models using lme4. *Journal of Statistical Software*, 67(1). <https://doi.org/10.18637/jss.v067.i01>
- Bender, M., Grande, K., Johnson, K., Marra, J., Williams, P. J. LeB., Sieburth, J., Pilson, M., Langdon, C., Hitchcock, G., Orchardo, J., Hunt, C., Donaghay, P., & Heinemann, K. (1987). A comparison of four methods for determining planktonic community production. *Limnology and Oceanography*, 32(5), 1085–1098. <https://doi.org/10.4319/lo.1987.32.5.1085>
- Bender, M., Orchardo, J., Dickson, M. L., Barber, R., & Lindley, S. (1999). In vitro O₂ fluxes compared with ¹⁴C production and other rate terms during the JGOFS Equatorial Pacific experiment. *Deep Sea Research Part I: Oceanographic Research Papers*, 46(4), 637–654. [https://doi.org/10.1016/S0967-0637\(98\)00080-6](https://doi.org/10.1016/S0967-0637(98)00080-6)
- Böttjer, D., Dore, J. E., Karl, D. M., Letelier, R. M., Mahaffey, C., Wilson, S. T., Zehr, J., & Church, M. J. (2017). Temporal variability of nitrogen fixation and particulate nitrogen export at Station ALOHA. *Limnology and Oceanography*, 62(1), 200–216. <https://doi.org/10.1002/lno.10386>
- Böttjer-Wilson, D., White, A., Björkman, K., Church, M., Poulos, S., Shimabukuro, E., Rii, Y., Ludwig, A., von Bröckel, K., Riebesell, U., Letelier, R., & Karl, D. (2021). Effects of nutrient enrichments on oligotrophic phytoplankton communities: a mesocosm experiment near Hawai‘i, USA. *Aquatic Microbial Ecology*, 87, 167–183. <https://doi.org/10.3354/ame01977>
- Brzezinski, M. A. (1985). The Si:C:N ratio of marine diatoms: Interspecific variability and the effect of some environmental variables. *Journal of Phycology*, 21(3), 347–357. <https://doi.org/10.1111/J.0022-3646.1985.00347.X>
- Church, M. J., Cullen, J. J., & Karl, D. M. (2019). Approaches to measuring marine primary production. In Cochran, J. Kirk; Bokuniewicz, J. Henry; Yager, L. Patricia (Eds.) *Encyclopedia of Ocean Sciences* (pp. 484–491). Elsevier. <https://doi.org/10.1016/B978-0-12-409548-9.11599-4>
- del Giorgio, P. A., & Williams, P. J. le B. (Eds) (2005). *Respiration in aquatic ecosystems*. Oxford University Press, USA.
- Dickson, M. L., & Orchardo, J. (2001). Oxygen production and respiration in the Antarctic Polar Front region during the austral spring and summer. *Deep Sea Research Part II: Topical Studies in Oceanography*, 48(19–20), 4101–4126. [https://doi.org/10.1016/S0967-0645\(01\)00082-0](https://doi.org/10.1016/S0967-0645(01)00082-0)
- Dickson, M. L., Orchardo, J., Barber, R. T., Marra, J., McCarthy, J. J., & Sambrotto, R. N. (2001). Production and respiration rates in the Arabian Sea during the 1995 Northeast and Southwest Monsoons. *Deep Sea Research Part II: Topical Studies in Oceanography*, 48(6–7), 1199–1230. [https://doi.org/10.1016/S0967-0645\(00\)00136-3](https://doi.org/10.1016/S0967-0645(00)00136-3)
- Dore, J. E., Brum, J. R., Tupas, L. M., & Karl, D. M. (2002). Seasonal and interannual variability in sources of nitrogen supporting export in the oligotrophic subtropical North Pacific Ocean. *Limnology and Oceanography*, 47(6), 1595–1607. <https://doi.org/10.4319/LO.2002.47.6.1595>

- Dore, J. E., Lukas, R., Sadler, D. W., Church, M. J., & Karl, D. M. (2009). Physical and biogeochemical modulation of ocean acidification in the central North Pacific. *Proceedings of the National Academy of Sciences of the United States of America*, *106*(30), 12235–12240. <https://doi.org/10.1073/PNAS.0906044106>
- Dore, J. E., Lukas, R., Sadler, D. W., & Karl, D. M. (2003). Climate-driven changes to the atmospheric CO₂ sink in the subtropical North Pacific Ocean. *Nature* *424*(6950), 754–757. <https://doi.org/10.1038/nature01885>
- Duarte, C. M., Regaudie-de-Gioux, A., Arrieta, J. M., Delgado-Huertas, A., & Agustí, S. (2013). The oligotrophic ocean is heterotrophic. *Annual Review of Marine Science*, *5*(1), 551–569. <https://doi.org/10.1146/annurev-marine-121211-172337>
- Ducklow, H. W., & Doney, S. C. (2013). What is the metabolic state of the oligotrophic ocean? A debate. *Annual Review of Marine Science*, *5*(1), 525–533. <https://doi.org/10.1146/annurev-marine-121211-172331>
- Dutkiewicz, S., Ward, B. A., Monteiro, F., & Follows, M. J. (2012). Interconnection of nitrogen fixers and iron in the Pacific Ocean: Theory and numerical simulations. *Global Biogeochemical Cycles*, *26*(1), GB1012. <https://doi.org/10.1029/2011GB004039>
- Dutkiewicz, S., Ward, B. A., Scott, J. R., & Follows, M. J. (2014). Understanding predicted shifts in diazotroph biogeography using resource competition theory. *Biogeosciences*, *11*, 5445–5461. <https://doi.org/10.5194/bg-11-5445-2014>
- Emerson, S. (2014). Annual net community production and the biological carbon flux in the ocean. *Global Biogeochemical Cycles*, *28*(1), 14–28. <https://doi.org/10.1002/2013GB004680>
- Falkowski, P. G. (1997). Evolution of the nitrogen cycle and its influence on the biological sequestration of CO₂ in the ocean. *Nature*, *387*(6630), 272–275. <https://doi.org/10.1038/387272A0>
- Falkowski, P. G., Dubinsky, Z., & Santostefano, G. (1985). Light-enhanced dark respiration in phytoplankton. *Societas Internationalis Limnologiae Proceedings 1922-2010*, *22*(5), 2830–2833. <https://doi.org/10.1080/03680770.1983.11897784>
- Falkowski, P. G., & Raven, J. A. (2007). Aquatic photosynthesis. 2nd Edition. *Blackwell Science, London, UK*, 484. <https://press.princeton.edu/books/paperback/9780691115511/aquatic-photosynthesis>
- Ferrón, S., del Valle, D. A., Björkman, K. M., Quay, P. D., Church, M. J., & Karl, D. M. (2016). Application of membrane inlet mass spectrometry to measure aquatic gross primary production by the ¹⁸O in vitro method. *Limnology and Oceanography: Methods*, *14*(9), 610–622. <https://doi.org/10.1002/lom3.10116>
- Field, C. B., Behrenfeld, M. J., Randerson, J. T., & Falkowski, P. (1998). Primary production of the biosphere: Integrating terrestrial and oceanic components. *Science*, *281*(5374), 237–240. <https://doi.org/10.1126/science.281.5374.237>
- Garcia, H. E., & Gordon, L. I. (1992). Oxygen solubility in seawater: Better fitting equations. *Limnology and Oceanography*, *37*(6), 1307–1312. <https://doi.org/10.4319/LO.1992.37.6.1307>
- Geider, R. J., & la Roche, J. (2002). Redfield revisited: variability of C:N:P in marine microalgae and its biochemical basis. *European Journal of Phycology*, *37*(1), 1–17. <https://doi.org/10.1017/S0967026201003456>
- Grabowski, M. N. W., Church, M. J., & Karl, D. M. (2008). Nitrogen fixation rates and controls at Stn ALOHA. *Aquatic Microbial Ecology*, *52*(2), 175–183. <https://doi.org/10.3354/AME01209>
- Gradoville, M. R., White, A. E., Böttjer, D., Church, M. J., & Letelier, R. M. (2014). Diversity trumps acidification: Lack of evidence for carbon dioxide enhancement of *Trichodesmium* community nitrogen or carbon fixation at Station ALOHA. *Limnology and Oceanography*, *59*(3), 645–659. <https://doi.org/10.4319/lo.2014.59.3.0645>
- Grande, K. D., Marra, J., Langdon, C., Heinemann, K., & Bender, M. L. (1989). Rates of respiration in the light measured in marine phytoplankton using an ¹⁸O isotope-labelling technique. *Journal of*

- Experimental Marine Biology and Ecology*, 129(2), 95–120. [https://doi.org/10.1016/0022-0981\(89\)90050-6](https://doi.org/10.1016/0022-0981(89)90050-6)
- Hamme, R. C., & Emerson, S. R. (2004). The solubility of neon, nitrogen and argon in distilled water and seawater. *Deep Sea Research Part I: Oceanographic Research Papers*, 51(11), 1517–1528. <https://doi.org/10.1016/J.DSR.2004.06.009>
- Henson, S. A., Sanders, R., Madsen, E., Morris, P. J., le Moigne, F., & Quartly, G. D. (2011). A reduced estimate of the strength of the ocean's biological carbon pump. *Geophysical Research Letters*, 38(4), L04606. <https://doi.org/10.1029/2011GL046735>
- Holmes, R. M., Aminot, A., K erouel, R., Hooker, B. A., & Peterson, B. J. (2011). A simple and precise method for measuring ammonium in marine and freshwater ecosystems. *Canadian Journal of Fisheries and Aquatic Sciences*, 56(10), 1801–1808. <https://doi.org/10.1139/F99-128>
- Kana, T. M. (1990). Light-dependent oxygen cycling measured by an oxygen-18 isotope dilution technique. *Marine Ecology Progress Series*, 64, 292–300. <https://doi.org/10.3354/meps064293>
- Kana, T. M., Darkangelo, C., Hunt, M. D., Oldham, J. B., Bennett, G. E., & Cornwell, J. C. (1994). Membrane inlet mass spectrometer for rapid high-precision determination of N₂, O₂, and Ar in environmental water samples. *Analytical Chemistry*, 66(23), 4188–4170. <https://doi.org/10.1021/ac00095a009>
- Karl, D., & Letelier, R. (2008). Nitrogen fixation-enhanced carbon sequestration in low nitrate, low chlorophyll seascapes. *Marine Ecology Progress Series*, 364, 257–268. <https://doi.org/10.3354/meps07547>
- Karl, D., Letelier, R., Tupas, L., Dore, J., Christian, J., & Hebel, D. (1997). The role of nitrogen fixation in biogeochemical cycling in the subtropical North Pacific Ocean. *Nature*, 388(6642), 533–538. <https://doi.org/10.1038/41474>
- Karl, D. M. (2000). Phosphorus, the staff of life. *Nature*, 406(6791), 31–33. <https://doi.org/10.1038/35017683>
- Karl, D. M., Bidigare, R. R., & Letelier, R. M. (2001). Long-term changes in plankton community structure and productivity in the North Pacific Subtropical Gyre: The domain shift hypothesis. *Deep Sea Research Part II: Topical Studies in Oceanography*, 48(8–9), 1449–1470. [https://doi.org/10.1016/S0967-0645\(00\)00149-1](https://doi.org/10.1016/S0967-0645(00)00149-1)
- Karl, D. M., Bj orkman, K. M., Dore, J. E., Fujieki, L., Hebel, D. v., Houlihan, T., Letelier, R. M., & Tupas, L. M. (2001). Ecological nitrogen-to-phosphorus stoichiometry at station ALOHA. *Deep Sea Research Part II: Topical Studies in Oceanography*, 48(8–9), 1529–1566. [https://doi.org/10.1016/S0967-0645\(00\)00152-1](https://doi.org/10.1016/S0967-0645(00)00152-1)
- Karl, D. M., & Church, M. J. (2014). Microbial oceanography and the Hawaii Ocean Time-series programme. *Nature Reviews Microbiology*, 12(10), 699–713. <https://doi.org/10.1038/nrmicro3333>
- Karl, D. M., Laws, E. A., Morris, P., Williams, P. J. L. B., & Emerson, S. (2003). Metabolic balance of the open sea. *Nature*, 426(6962), 32–32. <https://doi.org/10.1038/426032a>
- Karl, D. M., Letelier, R. M., Bidigare, R. R., Bj orkman, K. M., Church, M. J., Dore, J. E., & White, A. E. (2021). Seasonal-to-decadal scale variability in primary production and particulate matter export at Station ALOHA. *Progress in Oceanography*, 195, 102563. <https://doi.org/10.1016/J.POCEAN.2021.102563>
- Karl, D. M., & Lukas, R. (1996). The Hawaii Ocean Time-series (HOT) program: Background, rationale and field implementation. *Deep Sea Research Part II: Topical Studies in Oceanography*, 43(2–3), 129–156. [https://doi.org/10.1016/0967-0645\(96\)00005-7](https://doi.org/10.1016/0967-0645(96)00005-7)
- Karl, D., Michaels, A., Bergman, B., Capone, D., Carpenter, E., Letelier, R., Lipschultz, F., Paerl, H., Sigman, D., & Stal, L. (2002). Dinitrogen fixation in the world's oceans. *Biogeochemistry*, 57(1), 47–98. <https://doi.org/10.1023/A:1015798105851>

- Kroopnick, P., & Craig, H. (1972). Atmospheric oxygen: Isotopic composition and solubility fractionation. *Science*, *175*(4017), 54–55. <https://doi.org/10.1126/SCIENCE.175.4017.54>
- Kuznetsova, A., Brockhoff, P. B., & Christensen, R. H. B. (2017). lmerTest Package: Tests in Linear Mixed Effects Models. *Journal of Statistical Software*, *82*(13), 1–26. <https://doi.org/10.18637/jss.v082.i13>
- Lancelot, C., & Mathot, S. (1985). Biochemical fractionation of primary production by phytoplankton in Belgian coastal waters during short- and long-term incubations with ¹⁴C-bicarbonate. *Marine Biology*, *86*(3), 219–226. <https://doi.org/10.1007/BF00397507>
- Lenton, T. M., Boyle, R. A., Poulton, S. W., Shields-Zhou, G. A., & Butterfield, N. J. (2014). Co-evolution of eukaryotes and ocean oxygenation in the Neoproterozoic era. *Nature Geoscience*, *7*(4), 257–265. <https://doi.org/10.1038/ngeo2108>
- Letelier, R. M., Björkman, K. M., Church, M. J., Hamilton, D. S., Mahowald, N. M., Scanza, R. A., Schneider, N., White, A. E., & Karl, D. M. (2019). Climate-driven oscillation of phosphorus and iron limitation in the North Pacific Subtropical Gyre. *Proceedings of the National Academy of Sciences of the United States of America*, *116*(26), 12720–12728. <https://doi.org/10.1073/PNAS.1900789116>
- Lewitus, A. J., & Kana, T. M. (1995). Light respiration in six estuarine phytoplankton species: Contrasts under photoautotrophic and mixotrophic growth conditions. *Journal of Phycology*, *31*(5), 754–761. <https://doi.org/10.1111/j.0022-3646.1995.00754.x>
- Mahaffey, C., Björkman, K. M., & Karl, D. M. (2012). Phytoplankton response to deep seawater nutrient addition in the North Pacific Subtropical Gyre. *Marine Ecology Progress Series*, *460*, 13–34. <https://doi.org/10.3354/meps09699>
- Mahaffey, C., Reynolds, S., Davis, C. E., & Lohan, M. C. (2014). Alkaline phosphatase activity in the subtropical ocean: Insights from nutrient, dust and trace metal addition experiments. *Frontiers in Marine Science*, *1*(73). <https://doi.org/10.3389/fmars.2014.00073>
- Mantikci, M., Hansen, J. L. S., & Markager, S. (2017). Photosynthesis enhanced dark respiration in three marine phytoplankton species. *Journal of Experimental Marine Biology and Ecology*, *497*, 188–196. <https://doi.org/10.1016/J.JEMBE.2017.09.015>
- Mantikci, M., Staehr, P. A., Hansen, J. L. S., & Markager, S. (2019). Patterns of dark respiration in aquatic systems. *Marine and Freshwater Research*, *71*(4) 432–442. <https://doi.org/10.1071/MF18221>
- Markager, S., Jespersen, A.-M., Madsen, T. V., Berdalet, E., & Weisburd, R. (1992). Diel changes in dark respiration in a plankton community. In *The Daily Growth Cycle of Phytoplankton* (pp. 119–130). Springer Netherlands. https://doi.org/10.1007/978-94-011-2805-6_10
- Markager, S., & Sand-Jensen, K. (1989). Patterns of night-time respiration in a dense phytoplankton community under a natural light regime. *The Journal of Ecology*, *77*(1), 49–61. <https://doi.org/10.2307/2260915>
- Martiny, A. C., Pham, C. T. A., Primeau, F. W., Vrugt, J. A., Moore, J. K., Levin, S. A., & Lomas, M. W. (2013). Strong latitudinal patterns in the elemental ratios of marine plankton and organic matter. *Nature Geoscience* *2013 6:4*, *6*(4), 279–283. <https://doi.org/10.1038/ngeo1757>
- McAndrew, P. M., Björkman, K. M., Church, M. J., Morris, P. J., Jachowski, N., Williams, P. J. le B., & Karl, D. M. (2007). Metabolic response of oligotrophic plankton communities to deep water nutrient enrichment. *Marine Ecology Progress Series*, *332*, 63–75. <https://doi.org/10.3354/meps332063>
- Mesa, E., Delgado-Huertas, A., Carrillo-De-Albornoz, P., Garcia-Corral, L. S., Sanz-Martin, M., Wassmann, P., Reigstad, M., Sejr, M., Dalsgaard, T., & Duarte, C. M. (2017). Continuous daylight in the high-Arctic summer supports high plankton respiration rates compared to those supported in the dark. *Scientific Reports*, *7*(1), 1–8. <https://doi.org/10.1038/s41598-017-01203-7>

- Meyer, J., Löscher, C. R., Neulinger, S. C., Reichel, A. F., Loginova, A., Borchard, C., Schmitz, R. A., Hauss, H., Kiko, R., & Riebesell, U. (2016). Changing nutrient stoichiometry affects phytoplankton production, DOP accumulation and dinitrogen fixation—a mesocosm experiment in the eastern tropical North Atlantic. *Biogeosciences*, *13*, 781–794. <https://doi.org/10.5194/bg-13-781-2016>
- Mills, M. M., & Arrigo, K. R. (2010). Magnitude of oceanic nitrogen fixation influenced by the nutrient uptake ratio of phytoplankton. *Nature Geoscience*, *3*(6), 412–416. <https://doi.org/10.1038/ngeo856>
- Mills, M. M., Ridame, C., Davey, M., la Roche, J., & Geider, R. J. (2004). Iron and phosphorus co-limit nitrogen fixation in the eastern tropical North Atlantic. *Nature*, *429*(6989), 292–294. <https://doi.org/10.1038/nature02550>
- Moreno, A. R., & Martiny, A. C. (2018). Ecological Stoichiometry of Ocean Plankton. *Annual Review of Marine Science*, *10*(1), 43–69. <https://doi.org/10.1146/annurev-marine-121916-063126>
- Pringault, O., Tassas, V., & Rochelle-Newall, E. (2007). Consequences of respiration in the light on the determination of production in pelagic systems. *Biogeosciences*, *4*(1), 105–114. <https://doi.org/10.5194/bg-4-105-2007>
- Redfield, A. C. (1958). The biological control of chemical factors in the environment. *American Scientist*, *46*(3), 205–221. <https://www.jstor.org/stable/27827150>
- Roberts, B. J., & Howarth, R. W. (2006). Nutrient and light availability regulate the relative contribution of autotrophs and heterotrophs to respiration in freshwater pelagic ecosystems. *Limnology and Oceanography*, *51*(1), 288–298. <https://doi.org/10.4319/lo.2006.51.1.0288>
- Robinson, C., Tilstone, G. H., Rees, A. P., Smyth, T. J., Fishwick, J. R., Tarran, G. A., Luz, B., Barkan, E., & David, E. (2009). Comparison of in vitro and in situ plankton production determinations. *Aquatic Microbial Ecology*, *54*, 13–34. <https://doi.org/10.3354/ame01250>
- Robinson, C., & Williams, P. (2005). Respiration and its measurement in surface marine waters. In del Giorgio, P. A., & Williams, P. J. le B. (Eds) (2005). *Respiration in aquatic ecosystems* (pp. 147–180). Oxford University Press, USA.
- Schade, J. D., Espeleta, J. F., Klausmeier, C. A., McGroddy, M. E., Thomas, S. A., & Zhang, L. (2005). A conceptual framework for ecosystem stoichiometry: balancing resource supply and demand. *Oikos*, *109*(1), 40–51. <https://doi.org/10.1111/J.0030-1299.2005.14050.X>
- Shaffer, G. (1996). Biogeochemical cycling in the global ocean: 2. New production, Redfield ratios, and remineralization in the organic pump. *Journal of Geophysical Research: Oceans*, *101*(C2), 3723–3745. <https://doi.org/10.1029/95JC03373>
- Siegenthaler, U., & Sarmiento, J. L. (1993). Atmospheric carbon dioxide and the ocean. *Nature*, *365*(6442), 119–125. <https://doi.org/10.1038/365119a0>
- Sverdrup, H. U., Johnson, M. W., & Fleming, R. H. (1942). *The Oceans Their Physics, Chemistry, and General Biology*. Prentice-Hall.
- Taylor, B. W., Keep, C. F., Hall, R. O., Koch, B. J., Tronstad, L. M., Flecker, A. S., & Ulseth, A. J. (2007). Improving the fluorometric ammonium method: matrix effects, background fluorescence, and standard additions. *Journal of the North American Benthological Society*, *26*(2), 167–177. [https://doi.org/10.1899/0887-3593\(2007\)26\[167:ITFAMM\]2.0.CO;2](https://doi.org/10.1899/0887-3593(2007)26[167:ITFAMM]2.0.CO;2)
- Tilman, D., Kilham, S. S., & Kilham, P. (1982). Phytoplankton community ecology: The role of limiting nutrients. *Annual Review of Ecology and Systematics*, *13*(1), 349–372. <https://doi.org/10.1146/annurev.es.13.110182.002025>
- Tilman David. (1977). Resource competition between plankton algae: an experimental and theoretical approach. *Ecology*, *58*(2), 338–348. <https://doi.org/10.2307/1935608>
- Turk-Kubo, K. A., Connell, P., Caron, D., Hogan, M. E., Farnelid, H. M., & Zehr, J. P. (2018). In situ diazotroph population dynamics under different resource ratios in the North Pacific subtropical gyre. *Frontiers in Microbiology*, *9*(JUL), 1616. <https://doi.org/10.3389/fmicb.2018.01616>

- Ward, B. A., Dutkiewicz, S., Moore, C. M., & Follows, M. J. (2013). Iron, phosphorus, and nitrogen supply ratios define the biogeography of nitrogen fixation. *Limnology and Oceanography*, 58(6), 2059–2075. <https://doi.org/10.4319/lo.2013.58.6.2059>
- Watkins-Brandt, K. S., Letelier, R. M., Spitz, Y. H., Church, M. J., Böttjer, D., & White, A. E. (2011). Addition of inorganic or organic phosphorus enhances nitrogen and carbon fixation in the oligotrophic North Pacific. *Marine Ecology Progress Series*, 432, 17–29. <https://doi.org/10.3354/MEPS09147>
- Weber, T. S., & Deutsch, C. (2010). Ocean nutrient ratios governed by plankton biogeography. *Nature*, 467(7315), 550–554. <https://doi.org/10.1038/nature09403>
- White, A. E., Karl, D. M., Björkman, K. M., Beversdorf, L. J., & Letelier, R. M. (2010). Production of organic matter by *Trichodesmium* IMS101 as a function of phosphorus source. *Limnology and Oceanography*, 55(4), 1755–1767. <https://doi.org/10.4319/lo.2010.55.4.1755>
- Williams, P. J. le B., Quay, P. D., Westberry, T. K., & Behrenfeld, M. J. (2013). The oligotrophic ocean is autotrophic. *Annual Review of Marine Science*, 5(1), 535–549. <https://doi.org/10.1146/annurev-marine-121211-172335>
- Zehr, J. P., Montoya, J. P., Jenkins, B. D., Hewson, I., Mondragon, E., Short, C. M., Church, M. J., Hansen, A., & Karl, D. M. (2007). Experiments linking nitrogenase gene expression to nitrogen fixation in the North Pacific subtropical gyre. *Limnology and Oceanography*, 52(1), 169–183. <https://doi.org/10.4319/LO.2007.52.1.0169>

Appendix

Table A1: Institutions and teams that took part in PERI-FIX, along with their samples requested for analysis.

Institution	Team/Lab	Samples/Analysis
University of Southern California	John Lab (Lead)	Dissolved Trace Metals Inorganic N, P, and Si Particulate C, N, P, and Metals Dissolved Organic Carbon Total Dissolved N & P Chlorophyll
	Caron Lab	DNA & RNA genomics
University of Hawai‘i at Mānoa	HOT/SCOPE	Flow Cytometry
	White Lab	Imaging FlowCytobot
	Karl Lab	Nitrogen Fixation Acetylene Reduction Particulate P Particulate ATP Phosphate turnover
Dalhousie University	Finkel Lab	Total RNA/DNA Proteins Carbohydrates Lipids
Lamont-Doherty Earth Observatory	Dyhrman Lab	Metatranscriptomes Alkaline Phosphatase Activity
Woods Hole Oceanographic Institution	Repeta Lab	Dissolved Siderophores
	Van Mooy Lab	Lipidomics
University of California – Santa Cruz	Zehr Lab	<i>nifH</i> genes
University of Washington	Ingalls Lab	Metabolites

Complementary Measurements

As many as 12 laboratories and 35 sample types were collected during PERI-FIX, highlighting its collaborative nature (Table A1). For this research we have accessed the chlorophyll (Fig. A1) and inorganic nutrient (Fig. A4) datasets.

○ *Chlorophyll*

The chlorophyll dataset was created by Emily Townsend, Brendon Munoz, and Matt Strickland from the University of Southern California. Unfiltered water was collected in opaque 125-mL bottles for chlorophyll *a* (Chl) each day sampling was conducted, and later were filtered through GFF filters. The samples were extracted in 100% acetone (Acetone $\geq 99.3\%$) and stored at -20C for seven days before analysis on a Turner Designs Trilogy Laboratory Fluorometer using the Chl *a* Acidification Fluorescence module.

Chlorophyll *a* concentrations (Chl) show an immediate response in all treatments with added N, with concentrations increasing by up to six-fold by the end of the experiment compared to the first sampling day on August 11th. The increase in phytoplankton biomass was not gradual, but instead there was a boom two days after the first spike, and a crash produced by stopping nutrient spikes, with a gradual rise afterwards (Fig. A1). In contrast, the chlorophyll concentrations in the treatments with no inorganic N added were relatively constant with time except for the P and PF treatments that exhibited a late increase of about two- to three-fold in the last week of the experiment.

Chlorophyll

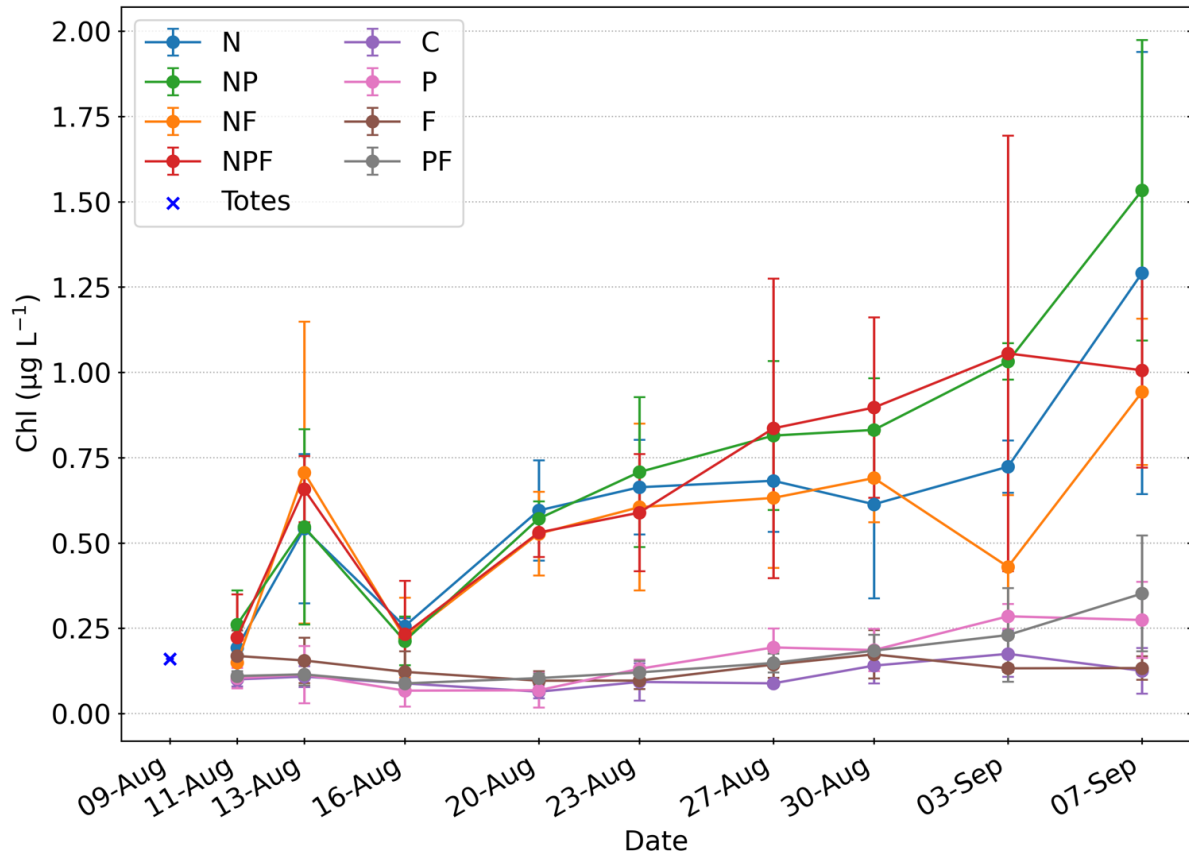


Figure A1: Plot of the daily means of Chlorophyll *a* concentrations in μg per liter for each treatment, with standard deviation as error bars ($n = 3$ tanks per treatment). The mean value for the totes on offshore collection date is also included.

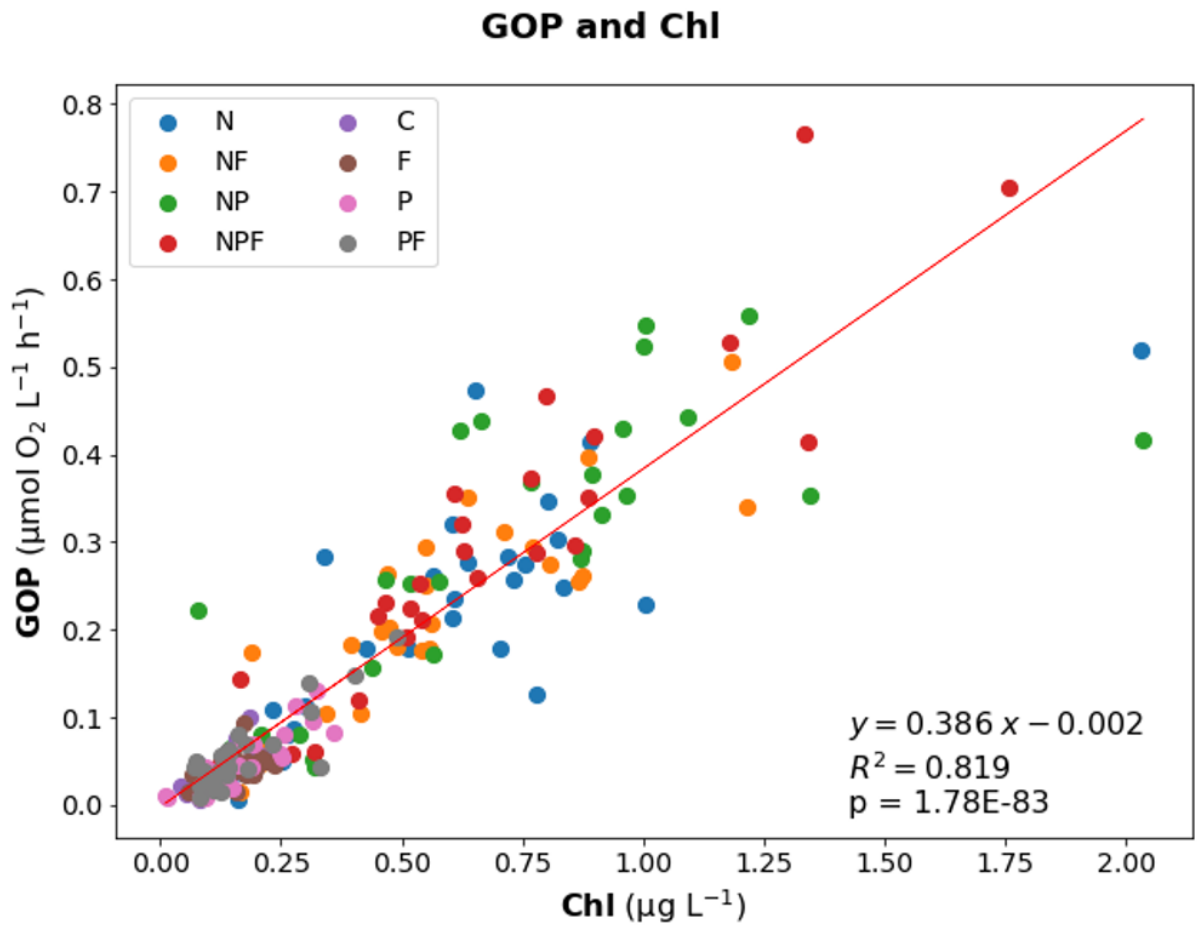


Figure A2: Plot of the correlation between GOP and chlorophyll, with a Model II linear regression line in red, the regression equation, R^2 value, and Pearson's correlation p-value.

GOP to Chl ratio
in $\mu\text{mol O}_2 (\mu\text{g Chl})^{-1} \text{h}^{-1}$

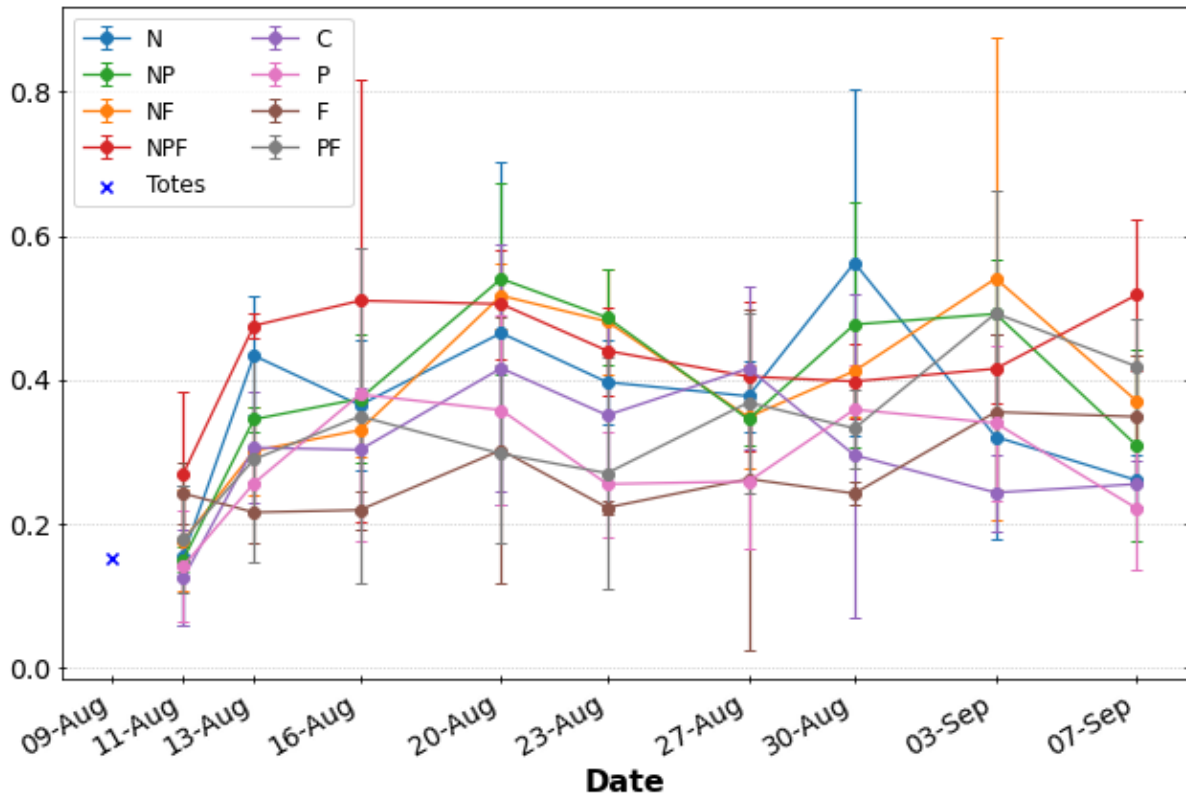


Figure A3: Plot of the daily means of GOP to Chl ratios in $\mu\text{mol O}_2 (\mu\text{g Chl})^{-1} \text{h}^{-1}$ for each treatment, with standard deviation as error bars ($n = 3$ tanks per treatment). The mean value for the totes on offshore collection date is also included as a blue cross.

○ *Inorganic Nutrients*

The inorganic nutrient dataset was created by Emily Townsend from the University of Southern California, along with Carolina Funkey and Rhea Foreman from the University of Hawai‘i at Mānoa. Sampling for Nitrate plus Nitrite (N+N), Soluble Reactive Phosphorus (SRP), Soluble Reactive Silica (SRSi), and ammonium were measured during the course of PERI-FIX. N+N, SRP, and SRSi were assessed colorimetrically with a 4-channel SEAL Analytical AA3 continuous flow system following the Hawai‘i Ocean Time-series protocols (hahana.soest.hawaii.edu/hot/protocols/protocols.html). Ammonium was assessed fluorometrically with a Turner Designs 10-AU Fluorometer using the methods described in Holmes et al. (2011) with modifications presented in Taylor et al. (2007).

Most of the nitrate and ammonium added—a total of 2.1 μmol each by the end of the experiment—was immediately consumed by the plankton community, with concentrations in all cases remaining below 0.2 μM for nitrate and 0.4 μM for ammonium despite the daily additions. During the first week, the concentrations of N+N in the treatments with N additions showed some residual above 0.15 μM , but after August 13th, the concentrations remained below 0.5 μM (Fig. A4A). Phosphate concentrations were similar for all treatments in the first few days of the experiment, but from the 11th of August onwards, some residual phosphate (greater than 0.1 μM) accumulated in the P and PF tanks while it decreased in all other treatments (Fig. A4B). In the last few days of the experiment, the P and PF tanks had a slight decrease in phosphate concentrations. Silica concentrations were highest in the first five days of the experiment for all treatments, but after that it was gradually consumed with concentrations decreasing below 0.4 μM in the tanks provided N (Fig. A4B)

Inorganic Nutrients in $\mu\text{mol L}^{-1}$

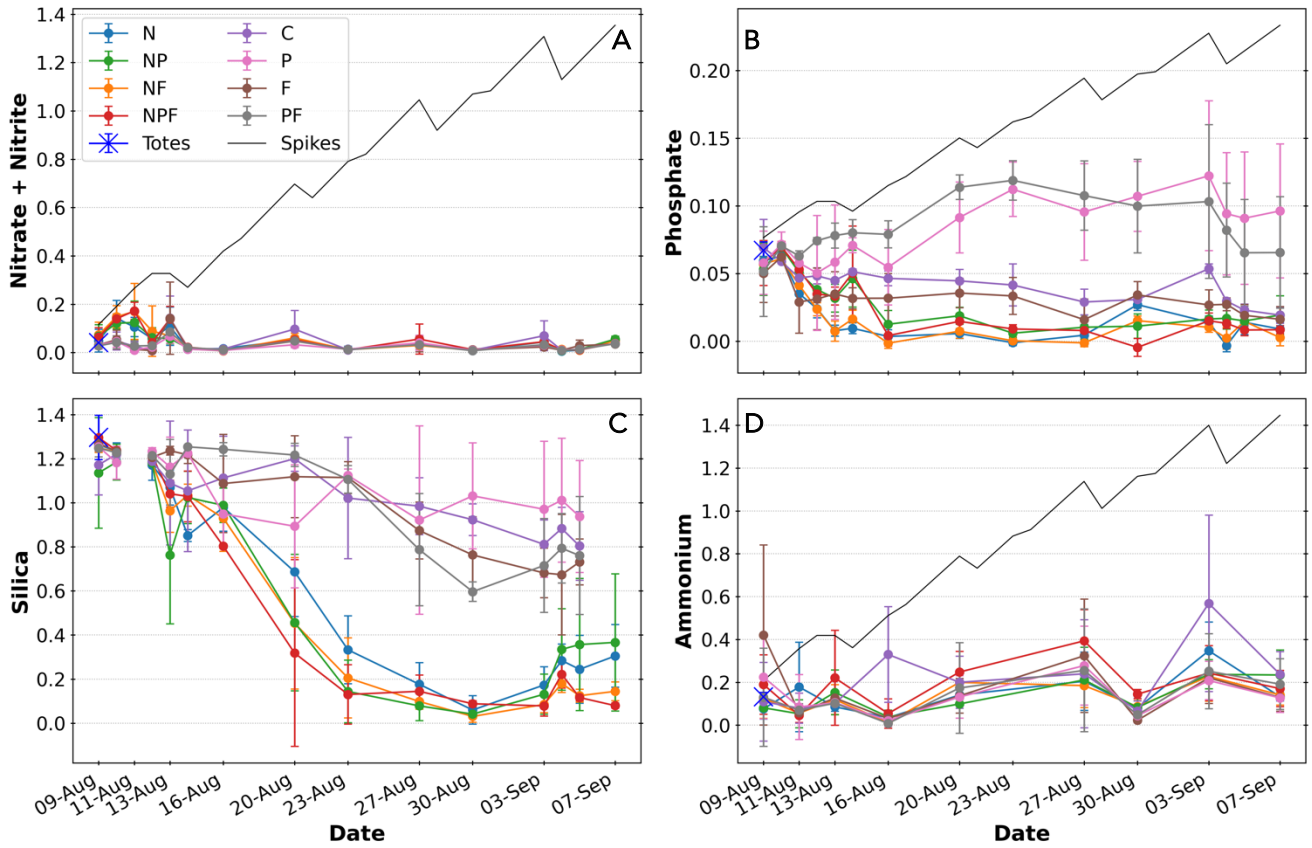


Figure A4: Plot of the daily means of inorganic nutrient concentrations for each treatment, with standard deviation as error bars ($n = 3$ tanks). **A)** Nitrate and nitrite, **B)** Phosphate, **C)** Silica, and **D)** Ammonium, all in μM units. The mean value with standard deviation for the totes on offshore collection date are also included as blue crosses. The gray line indicates the cumulative addition from the nutrient spikes, accounting for sampling dilutions.